THE JOURNAL OF BIOLOGICAL CHEMISTRY VOL. 287, NO. 45, pp. 38135–38149, November 2, 2012


# Domain Organization of the Polymerizing Mannosyltransferases Involved in Synthesis of the *Escherichia coli* O8 and O9a Lipopolysaccharide O-antigens*[S]

Received for publication, August 21, 2012, and in revised form, September 16, 2012 Published, JBC Papers in Press, September 18, 2012, DOI 10.1074/jbc.M112.412577

**Laura K. Greenfield[‡1], Michele R. Richards[§2], Evgeny Vinogradov[¶], Warren W. Wakarchuk[¶3], Todd L. Lowary[§], and Chris Whitfield[‡4]**

*From the [‡]Department of Molecular and Cellular Biology, University of Guelph, Guelph, Ontario N1G 2W1, the [§]Alberta Glycomics Centre and Department of Chemistry, University of Alberta, Edmonton, Alberta T6G 2G2, and the [¶]Institute for Biological Sciences, National Research Council of Canada, Ottawa, Ontario K1A 0R6, Canada*

**Background:** *Escherichia coli* O8 and O9a polysaccharide repeat units are synthesized by serotype-specific multidomain (WbdA) mannosyltransferases.
**Results:** The various WbdA domains are functional when expressed individually.
**Conclusion:** The number of domains identified in each WbdA protein correlates with the different linkage types formed by the enzyme.
**Significance:** Modular glycosyltransferases could be exploited for synthesis of precise glycoconjugates with medical and industrial applications.

**The *Escherichia coli* O9a and O8 polymannose O-polysaccharides (O-PSs) serve as model systems for the biosynthesis of bacterial polysaccharides by ATP-binding cassette transporter-dependent pathways. Both O-PSs contain a conserved primer-adaptor domain at the reducing terminus and a serotype-specific repeat unit domain. The repeat unit domain is polymerized by the serotype-specific WbdA mannosyltransferase. In serotype O9a, WbdA is a bifunctional $\alpha$-(1→2)-, $\alpha$-(1→3)-mannosyltransferase, and its counterpart in serotype O8 is trifunctional ($\alpha$-(1→2), $\alpha$-(1→3), and $\beta$-(1→2)). Little is known about the detailed structures or mechanisms of action of the WbdA polymerases, and here we establish that they are multidomain enzymes. WbdA$^{O9a}$ contains two separable and functionally active domains, whereas WbdA$^{O8}$ possesses three. In WbdC$^{O9a}$ and WbdB$^{O9a}$, substitution of the first Glu of the E$X_7$E motif had detrimental effects on the enzyme activity, whereas substitution of the second had no significant effect on activity *in vivo*. Mutation of the Glu residues in the E$X_7$E motif of the N-terminal WbdA$^{O9a}$ domain resulted in WbdA variants unable to synthesize O-PS. In contrast, mutation of the Glu residues in the motif of the C-terminal WbdA$^{O9a}$ domain generated an enzyme capable of synthesizing an altered O-PS repeat unit consisting of only $\alpha$-(1→2) linkages. *In vitro* assays with synthetic acceptors unequivocally confirmed that the N-terminal domain of WbdA$^{O9a}$ possesses $\alpha$-(1→2)-mannosyltransferase activity. Together, these studies form a framework for detailed structure-function studies on individual domains and a strategy applicable for dissection and analysis of other multidomain glycosyltransferases.**

Lipopolysaccharides (LPSs) are unique glycolipids that represent major and characteristic components of outer membranes in Gram-negative bacteria. In enteric bacteria, the hydrophobic anchor of LPS, lipid A, is linked via a core oligosaccharide to a hypervariable long-chain repeat unit polysaccharide (1). Variations in the structures of the polysaccharide repeat units define more than 180 different O-antigen serotypes in *Escherichia coli* (2, 3) and give rise to the term O-polysaccharide (O-PS).[5] The lipid A-core oligosaccharide portion of the molecule is synthesized independently of the O-PS, and the pathways converge with a ligation reaction that joins these components at the periplasmic face of the cytoplasmic membrane (1). The completed LPS molecules are then translocated to the outer leaflet of the outer membrane (reviewed in Ref. 4).

The O-PSs of *E. coli* O9, O9a, and O8 are a family of related structures comprising linear homopolymers of mannopyranose (Man*p*) (Fig. 1) (3). These glycans are prototypes for O-PSs synthesized via the well distributed ATP-binding cassette transporter-dependent pathway (5, 6). Their synthesis involves biosynthetic intermediates built on the 55-carbon polyisoprenoid lipid acceptor, undecaprenol phosphate. The pathway begins with the formation of und-PP-Glc*p*NAc by WecA (7–9).

* This work was supported in part by grants from the Natural Sciences and Engineering Research Council (to C. W. and T. L. L.) and by the Alberta Glycomics Centre (to T. L. L.)
[S] This article contains supplemental Table S1.
[1] Recipient of an Alexander Graham Bell Canada Graduate Scholarship from the Natural Sciences and Engineering Research Council.
[2] Recipient of an Alberta Innovates Health Solutions Ph.D. Studentship.
[3] Present address: Dept. of Chemistry and Biology, Ryerson University, 350 Victoria St., Toronto, Ontario M5B 2K3, Canada.
[4] Tier 1 Canada Research Chair. To whom correspondence should be addressed: Dept. of Molecular and Cellular Biology, Science Complex, University of Guelph, Guelph, Ontario N1G 2W1, Canada. Tel.: 519-824-4120 (ext. 53361); Fax: 519-837-3273; E-mail: cwhitfie@uoguelph.ca.

[5] The abbreviations used are: O-PS, O-polysaccharide; und-PP, undecaprenol pyrophosphate; LB, lysogeny broth; Man, mannose; Man*p*, mannopyranose; Glc*p*NAc, *N*-acetylglucosamine; MalE, maltose-binding protein; gCOSY, gradient-enhanced correlation spectroscopy; tROESY, transverse rotating frame Overhauser enhancement spectroscopy; gHSQC, gradient-enhanced heteronuclear single quantum correlation; BisTris, 2-[bis(2-hydroxyethyl)amino]-2-(hydroxymethyl)propane-1,3-diol.

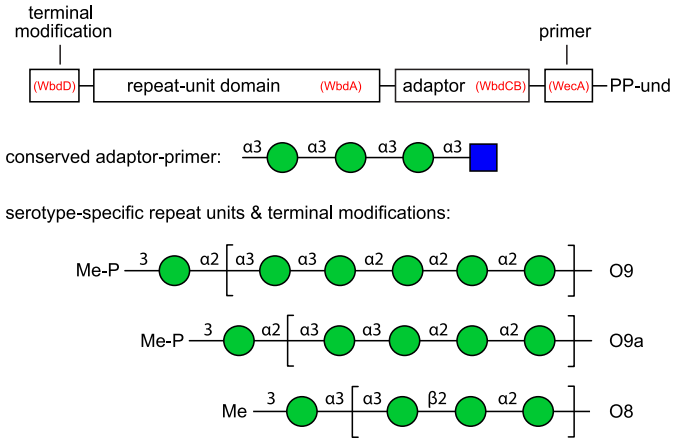


FIGURE 1. **Structures the *E. coli* O8, O9 and O9a polymannose O-PSs.** Each polysaccharide contains four structural regions, the primer, adaptor, repeat unit domain, and terminal modification, which are represented in the schematic in the context of the und-PP-linked biosynthetic intermediate. Glc*p*NAc is represented by a *blue square* and Man*p* by a *green circle* according to the nomenclature used by the Consortium for Functional Glycomics. The enzymes responsible for the formation of each part of the glycan are identified in *parentheses*.

WecA is part of the machinery for biosynthesis of the enterobacterial common antigen glycan (10) and initiates the formation of many different *E. coli* O-PS structures (11). The first dedicated activity in O8/O9/O9a biosynthesis involves transfer of a single α-(1→3)-linked Man*p* residue by the GDP-Man*p*-dependent mannosyltransferase, WbdC. Next, WbdB adds two α-(1→3)-linked Man*p* residues. The WbdCB enzymes are conserved and possess the same activities in all three serotypes (12, 13). Further chain extension builds the repeat unit domain of the O-PSs, and this is achieved by serotype-specific WbdA enzymes (13). The growing chains are terminated by methyl (O8) or phosphomethyl (O9/O9a) groups, which are added by the WbdD proteins. $WbdD^{O8}$ is a membrane-associated methyltransferase, whereas $WbdD^{O9/O9a}$ is a bifunctional kinase-methyltransferase (14, 15). The terminated glycan is then recognized by a serotype-specific carbohydrate-binding module located at the C terminus of the nucleotide-binding domain component of the ATP-binding cassette transporter, which defines this type of assembly pathway (16). Chain termination is essential for recognition and export (16).

The *E. coli* O9a and O8 O-PSs are identical to the *Klebsiella pneumoniae* O3 and O5 O-PSs, respectively (17–22), and the genetic loci encoding the corresponding O-PS biosynthesis enzymes are highly conserved (21). Detailed structural studies of the *K. pneumoniae* O3 and O5 O-PSs reveal conserved reducing termini and terminating residues that cap the variable serotype-specific repeat unit domains. These structural features are consistent with the assigned biochemical activities of the biosynthetic enzymes (Fig. 1) (15, 22, 23).

The NCBI Conserved Domain Database (24) predicts two putative glycosyltransferase domains in $WbdA^{O9a}$ and three in $WbdA^{O8}$. Each of these domains is predicted to encompass a retaining mannosyltransferase belonging to glycosyltransferase family GT4 in the CAZy Database (25).[6] Consistent with these predictions, the WbdA proteins are considerably larger than a typical single-active site enzyme, such as WbdB (43.9 kDa). $WbdA^{O9a}$ and $WbdA^{O8}$ have predicted sizes of 95.5 and 137 kDa, respectively. Interestingly, the number of glycosyltransferase domains predicted for each of the WbdA homologues is correlated with the number of different linkage types catalyzed by each enzyme. Previous studies proposed that $WbdA^{O9a}$ contained duplicated domains and showed that the domains could be separated, but both were required for O9a biosynthesis (26). Here, we show that $WbdA^{O8}$ is also a modular enzyme. It is currently unknown whether a specific functional mannosyltransferase activity is associated with each domain. We address this question in $WbdA^{O9a}$ by assessing the activities of proteins with mutated residues in catalytic site motifs that are conserved in GT4 enzymes, and we establish that the purified N-terminal domain of $WbdA^{O9a}$ possesses poly-α-(1→2)-mannosyltransferase activity.

## EXPERIMENTAL PROCEDURES

*Bacterial Strains, Plasmids, and Growth Conditions*—The bacterial strains and plasmids used in this study are described in Table 1. Bacteria were routinely grown in lysogeny broth (LB) medium (27). D-Glucose (0.4%, w/v), D-mannose (0.1%, w/v), L-arabinose (0.2%, w/v), isopropyl β-D-1-thiogalactopyranoside (0.5 mM), kanamycin (50 μg/ml), ampicillin (100 μg/ml), or chloramphenicol (34 μg/ml) was added where appropriate.

*General DNA Methods*—InstaGene Matrix (Bio-Rad) or DNAzol reagent (Invitrogen) was used to purify chromosomal DNA. DNA fragments were PCR-amplified using Pwo DNA polymerase (Roche Applied Science) or PfuUltra High-Fidelity DNA polymerase (Stratagene), using custom oligonucleotide primers (Sigma) containing restriction sites to facilitate cloning. The sequences and features of the oligonucleotide primers are described in supplemental Table S1. The PureLink PCR Purification Kit (Invitrogen) was used to purify DNA fragments from PCRs or restriction digestions, and DNA fragments from agarose gels were purified using the PureLink Quick Gel Extraction Kit (Invitrogen). Plasmid DNA was purified using the PureLink Quick Plasmid Miniprep Kit (Invitrogen). Restriction endonucleases (Invitrogen and New England Biolabs) and T4 DNA ligase (New England Biolabs) were used according to the manufacturer's instructions. DNA sequencing was performed by the Genomics Facility in the Advanced Analysis Centre (University of Guelph).

*Bioinformatic Analyses*—Multiple sequence alignments were generated using the ClustalW2 server available at the European Bioinformatics Institute Web site (28, 29). Secondary structure predictions were made using the online programs, JPred (30), PROF (31), SCRATCH Protein Predictor (SSPro) (32), and the PSIPRED Protein Structure Prediction Server (33, 34). Secondary structure models were generated based on the consensus of at least three of the secondary structure predictions. Conserved domain predictions were carried out using the NCBI Conserved Domain Database (24, 35, 36). Three-dimensional structural models were created using the Phyre2 server (37).

*Generation of Mannosyltransferase Constructs*—Segments of the O9a and O8 *wbdA* genes corresponding to the putative mannosyltransferase domains were PCR-amplified from *E. coli* CWG634 (O9a) and CWG636 (O8) chromosomal DNA and

[6] B. Henrissat, personal communication.

**TABLE 1**
**Bacterial strains and plasmids**

| Strain/plasmid | Description or genotype | Reference or source |
|---|---|---|
| **Strains** | | |
| Top10 | *E. coli* F$^-$, *mcrA*, Δ (*mrr-hsdRMS-mcrBC*), $\phi$80, *lacZ*ΔM15, Δ*lacX74*, *deoR*, *nupG*, *recA1*, *araD139*, Δ(*ara-leu*)7697, *galU*, *galK*, *repsL*(Str$^r$), *endA1* | Invitrogen |
| CWG634 | *E. coli* O9a:K$^-$; *trp his lac rpsL cps*$_{K30}$; *manA*; Sm$^r$; Tc$^r$ | Ref. 14 |
| CWG636 | *E. coli* O8:K$^-$; *ugd*::*aacC1 manA*; Gm$^r$; Tc$^r$ | Ref. 14 |
| CWG901 | *E. coli* O9a:K$^-$ derivative: *trp his lac rpsL cps*$_{K30}$ *manA* Δ*wbdA*::*aacC1*; Sm$^r$; Tc$^r$; Gm$^r$ | Ref. 64 |
| CWG1009 | *E. coli* O9a:K$^-$ derivative: *trp his lac rpsL cps*$_{K30}$ *manA* Δ*wbdB*; Sm$^r$; Tc$^r$ | Ref. 14 |
| CWG1010 | *E. coli* O9a:K$^-$ derivative: *trp his lac rpsL cps*$_{K30}$ *manA* Δ*wbdC*; Sm$^r$; Tc$^r$ | Ref. 13 |
| CWG1104 | *E. coli* O8:K$^-$ derivative: *ugd*::*aacC1 manA* Δ*wbdA*; Gm$^r$; Tc$^r$ | Ref. 13 |
| CWG1105 | *E. coli* O9a:K$^-$ derivative: *manA* Δ*wbdA*; Sm$^r$; Tc$^r$ | Ref. 13 |
| **Plasmids** | | |
| pBAD24 | Vector containing L-arabinose-inducible promoter; Ap$^r$ | Ref. 86 |
| pYA3265 | Source of non-polar *aphA-3* cassette; Km$^r$ | A. Honeyman via E. Vimr, Ref. 87 |
| pWQ284 | pBAD24 derivative containing a selectable Cm resistance marker; Cm$^r$ | Ref. 16 |
| pWQ573 | pWQ284 derivative; NcoI site in *cat* gene removed; XbaI in MCS replaced by SpeI; Cm$^r$ | J. King |
| pWQ575 | pMAL-c2X derivative containing an XmnI/HindIII fragment encoding WbdC$^{O9a}$; Ap$^r$ | Ref. 13 |
| pWQ576 | pMALc-2X derivative containing an EcoRI/HindIII fragment encoding WbdB$^{O9a}$; Ap$^r$ | Ref. 13 |
| pWQ583 | pWQ575 derivative containing WbdC$^{O9a}$ E275A mutation; Ap$^r$ | This study |
| pWQ584 | pWQ575 derivative containing WbdC$^{O9a}$ E283A mutation; Ap$^r$ | This study |
| pWQ585 | pWQ576 derivative containing WbdB$^{O9a}$ E294A mutation; Ap$^r$ | This study |
| pWQ586 | pWQ576 derivative containing WbdB$^{O9a}$ E302A mutation; Ap$^r$ | This study |
| pWQ589 | pBAD24 derivative containing a Km resistance cassette; Km$^r$ | B. Clarke |
| pWQ590 | pBAD24 derivative containing an EcoRI/HindIII fragment encoding His$_{10}$-WbdA$_{1–435}^{O9a}$; Ap$^r$ | This study |
| pWQ591 | pWQ284 derivative containing an EcoRI/HindIII fragment encoding His$_{10}$-WbdA$_{426–840}^{O9a}$; Cm$^r$ | This study |
| pWQ592 | pBAD24 derivative containing an NcoI/SpeI fragment encoding WbdA$_{1–450}^{O8}$; Ap$^r$ | This study |
| pWQ593 | pWQ573 derivative containing an *Nco*I/*Spe*I fragment encoding WbdA$_{1–450}^{O8}$; Cm$^r$ | This study |
| pWQ594 | pBAD24 derivative containing an NcoI/SpeI fragment encoding WbdA$_{615–1213}^{O8}$; Ap$^r$ | This study |
| pWQ595 | pWQ573 derivative containing an NcoI/SpeI fragment encoding WbdA$_{1–865}^{O8}$; Cm$^r$ | This study |
| pWQ596 | pWQ573 derivative containing an NcoI/SpeI fragment encoding WbdA$_{411–1213}^{O8}$; Cm$^r$ | This study |
| pWQ597 | pWQ631 derivative containing WbdA$^{O9a}$ E317A mutation; Km$^r$ | This study |
| pWQ598 | pWQ631 derivative containing WbdA$^{O9a}$ E325A mutation; Km$^r$ | This study |
| pWQ599 | pWQ631 derivative containing WbdA$^{O9a}$ E750A mutation; Km$^r$ | This study |
| pWQ630 | pWQ631 derivative containing WbdA$^{O9a}$ E758A mutation; Km$^r$ | This study |
| pWQ631 | pWQ589 derivative containing WbdD$_{475–708}$WbdA$^{O9a}$; Km$^r$ | B. Clarke |
| pWQ632 | pBAD24 derivative containing an EcoRI/HindIII fragment encoding His$_{10}$-WbdA$_{426–840}^{O9a}$; Ap$^r$ | This study |

cloned behind the arabinose-inducible promoter in pBAD24, pWQ284, or pWQ573, using restriction sites introduced by the oligonucleotide primers. To generate pWQ631, *wbdA*$^{O9a}$ was PCR-amplified from CWG634 and inserted into pWQ589. The PCR-amplified DNA fragment corresponding to the C terminus of WbdD (amino acids 475–708) was then inserted upstream of the *wbdA* gene. Site-directed mutagenesis of E$X_7$E motifs was carried out using the QuikChange method (Stratagene, La Jolla, CA). Briefly, mutations were introduced into plasmids via PCR using oligonucleotide primers incorporating the desired base changes (supplemental Table S1). The PCR products were digested with DpnI and transformed into *E. coli* Top10. All constructs were confirmed by restriction endonuclease digestion and/or by sequencing.

*Purification of Polyhistidine-tagged WbdA*$^{O9a}$ *Domains*—Cultures (500 ml) of *E. coli* Top10 containing pWQ590 (encoding N-WbdA$^{O9a}$) or pWQ632 (C-WbdA$^{O9a}$) were grown in LB medium at 37 °C until an $A_{600}$ of ~0.3 was reached. Cultures were transferred to 20 °C and grown until midexponential phase ($A_{600}$ = 0.6). Recombinant protein expression was then induced overnight at 20 °C by the addition of 0.2% arabinose. Cells were collected by centrifugation and resuspended in 25 ml of buffer A (20 mM BisTris, pH 7.0, 250 mM NaCl, 0.5% (w/v) glycerol), prior to lysis by sonication with intermittent cooling on ice. Unbroken cells and large debris were removed by centrifugation at 12,000 × *g* for 20 min, and the resulting cell-free lysate was centrifuged at 100,000 × *g* for 60 min to separate the membrane and soluble fractions. Protein purifications were performed by fast protein liquid chromatography (FPLC) using an ÄKTA Explorer system (GE Healthcare). Soluble material from the cell-free lysate was loaded onto a 5-ml HiTrap chelating HP column (Amersham Biosciences) charged with nickel ions. The column was washed sequentially with 3 column volumes of buffer A containing 0, 50, and 75 mM imidazole. N-WbdA$^{O9a}$ and C-WbdA$^{O9a}$ were eluted in buffer A containing 125 mM imidazole. The protein-containing fractions were pooled, and the buffer was exchanged with storage buffer (20 mM BisTris, pH 7.0, 50 mM NaCl), using a desalting column (GE Healthcare) according to the manufacturer's instructions. The samples were then concentrated using a 30,000 MWC Vivaspin filtration unit (Sartorius Biolab Products) according to the manufacturer's instructions. The protein concentrations were determined using the $A_{280}$, based on theoretical extinction coefficients of His$_{10}$-N-WbdA$^{O9a}$ (42,080 M$^{-1}$ cm$^{-1}$) and His$_{10}$-C-WbdA$^{O9a}$ (81,150 M$^{-1}$ cm$^{-1}$) predicted by the ProtParam program (38). The protein concentrations of His$_{10}$-N-WbdA$^{O9a}$ and His$_{10}$-C-WbdA$^{O9a}$ were typically 2 mg/ml.

*Structural Analysis of the O-PS Produced in Cells Containing Mutations in the C-terminal E$X_7$E Motif of WbdA*$^{O9a}$—The LPS from CWG901 (pWQ599 expressing WbdA E750A) was purified from 18 liters of culture according to the hot aqueous-phenol method described by Westphal and Jann (39). The polysaccharide was released from LPS by mild acid hydrolysis (2% acetic acid, 100 °C, 3 h), isolated by gel filtration chromatography as described elsewhere (22), and analyzed by NMR spectroscopy. Spectra for DQCOSY, TOCSY (mixing time 120 ms), NOESY (400 ms delay), and gHSQC experiments were obtained on a Varian Unity 500 NMR spectrometer in $D_2O$ at

25 °C. Standard pulse sequences were applied with reference to internal acetone ($^1$H, 2.23 ppm; $^{13}$C, 31.45 ppm). The AQ time was maintained at 0.8 s for H-H correlations and 0.25 s for gHSQC. 256 data series were collected for all spectra.

*In Vitro Mannosyltransferase Reactions Using Synthetic Acceptors*—Two synthetic fluorescein-tagged acceptors were used as substrates for N-WbdA$^{O9a}$ and C-WbdA$^{O9a}$. Acceptor A (α-Man*p*-(1→2)-α-Man*p*-(1→2)-α-Man*p*-(1→3)-α-Man*p*) represents the repeat unit of the O9a antigen. Acceptor B (α-Man*p*-(1→3)-α-Man*p*-(1→3)-β-Glc*p*NAc) represents the conserved reducing terminal trisaccharide of the O8 and O9a antigens. Their synthesis has been described elsewhere (15, 40, 41), and they have been used to characterize the WbdD$^{O9a}$-mediated chain-terminating activity (15) as well as activities of the full-length WbdA$^{O9a}$ and WbdA$^{O8}$ mannosyltransferases (13). Standard reactions were performed as described previously (13) in 10-μl reaction volumes of buffer B (50 mM HEPES, 20 mM $MgCl_2$, 1 mM dithiothreitol, pH 7.5) containing 10 μM enzyme (purified N-WbdA$^{O9a}$, C-WbdA$^{O9a}$, or both), 0.5 mM acceptor, and 5 mM GDP-Man*p*. Reactions were incubated for 30 min at 25 °C and terminated by the addition of an equal volume of stop solution (50% (v/v) acetonitrile, 1% (w/v) SDS, 10 mM EDTA). After diluting 1:4 in 50% (v/v) aqueous acetonitrile, 2-μl portions were spotted on AL SIL G thin layer chromatography plates (Whatman). The plates were developed with ethyl acetate/water/1-butanol/acetic acid (5:4:4:2.5), and fluorescent reaction products were detected with a hand-held UV lamp.

*Structural Analyses of Reaction Products*—To generate sufficient quantities of product for NMR spectroscopic analyses, 250-μl reactions were carried out as described above using Acceptor B. After 30 min, the reactions were diluted in 1 ml of $H_2O$ and loaded onto a $C_{18}$ Sep-Pak cartridge (Waters). The cartridge was washed extensively with water, and the products were eluted in 2 ml of 60% (v/v) aqueous acetonitrile. The eluted products were then concentrated using a SpeedVac concentrator. MALDI-TOF mass spectra of the reaction products were obtained on a Bruker Ultraflextreme MALDI-TOF/TOF in positive ion mode. All NMR spectra were acquired in $D_2O$ at 27 °C on an Agilent VNMRS 700-MHz spectrometer equipped with a cryoprobe. The spectra were referenced to an external standard of acetone (2.22 ppm for $^1$H and 31.07 ppm for $^{13}$C at 27 °C). One-dimensional, gCOSY and tROESY, $^1$H spectra were obtained for the products generated by N-WbdA$^{O9a}$ alone and by N-WbdA$^{O9a}$ and C-WbdA$^{O9a}$ together. Additionally, a $^1$H-$^{13}$C gHSQC spectrum was obtained for the products generated by N-WbdA$^{O9a}$ alone. For all of the $^1$H spectra, the intensity of the residual HOD peak was decreased using a presaturation pulse sequence, irradiating at 4.76 ppm. The spectral window for the one-dimensional $^1$H spectra was 8446 Hz (from 10.8 to −1.3 ppm), and a Gaussian function was applied interactively to improve the signal/noise ratio. The spectral windows for the gCOSY and tROESY were 6313 Hz (from 9.5 to 0.5 ppm) in both dimensions. The gCOSY was acquired with 674 increments in F1 and 8 transients in F2, and the tROESY was acquired with 600 increments in F1, 16 transients in F2, and a 0.4 s mixing time. The spectral window for the $^1$H-$^{13}$C gHSQC was 5605 Hz (from 9.0 to 1.0 ppm) in F2 ($^1$H dimension, 16 transients) and 28.2 kHz (from 160 to 0 ppm) in F1 ($^{13}$C dimension, 432 increments). The proton signals were decoupled during acquisition, and the $^1J_{C,H}$ value was set to 140 Hz to determine the appropriate delays. For all of the two-dimensional spectra, sine-bell functions were applied interactively to improve signal/noise ratio.

*Protein and LPS PAGE*—LPS samples were prepared by proteinase K digestion of whole-cell lysates according to the method of Hitchcock and Brown (42). Protein and LPS samples were analyzed by SDS-PAGE in Tris-glycine buffer (43). Protein was visualized using Simply Blue stain (Invitrogen), and LPS was visualized by silver staining (44). Western immunoblots of LPS were prepared by transferring samples to PROTRAN nitrocellulose membranes (PerkinElmer Life Sciences). Samples were probed at a 1:500 dilution with O9a-specific antiserum (14). Alkaline phosphatase-conjugated goat anti-rabbit secondary antibody (Cedar Lane Laboratories) was used at a dilution of 1:3000, and nitro blue terazolium and 5-bromo-4-chloro-3-indolyl phosphate (Roche Applied Science) were used as substrates for detection.

## RESULTS

*Modular Architecture of WbdA (Poly)Mannosyltransferase Proteins*—WbdC, WbdB, and each WbdA domain (from both O8 and O9a serotypes) are classified into the CAZy GT4 family of glycosyltransferases (25). To determine the boundaries for multiple mannosyltransferase domains in the WbdA proteins, an alignment was performed with PimA from mycobacteria. PimA is a single-active site GDP-Man*p*-dependent mannosyltransferase belonging to GT4 that is involved in the biosynthesis of phosphoinositol mannosides (45) and was chosen because its structure has been solved (46). The alignment revealed generally low sequence similarity between the various domains and PimA (Fig. 2). However, the two domains of WbdA$^{O9a}$ and two of three domains of WbdA$^{O8}$ possess a conserved region that includes an E$X_7$E motif found in other retaining glycosyltransferases, including GT4 members (47).[6] All but one (WsaF) of the 14 GT4 crystal structures, which includes viral, archaeal, prokaryotic, and eukaryotic representatives, show this motif within the active site of the enzyme, where it is known or predicted to be involved in binding of the nucleotide sugar donor (46, 48–57). The absence of this motif from one domain of WbdA$^{O8}$ makes it a candidate for the inverting glycosyltransferase activity associated with the O8 mannosyltransferase, adding the β-(1→2)-linked Man*p* residue in the O8 repeat unit (Fig. 1). The E$X_7$E motif is also present in WbdC and WbdB. The predicted secondary structure of each of the putative WbdA domains was compared with the secondary structure of PimA (determined from its crystal structure (46)). All five WbdA domains have predicted secondary structures similar to that of PimA (data not shown). Collectively, these analyses identified potential boundaries for the domains (Fig. 3) as well as a structural basis for generating constructs expressing the various domains singly or in combination.

Both WbdA$^{O9a}$ domains show features of a catalytically active glycosyltransferase module (*i.e.* they possess an E$X_7$E motif and share similar (predicted) secondary structures with PimA). To provide additional insight, three-dimensional mod-

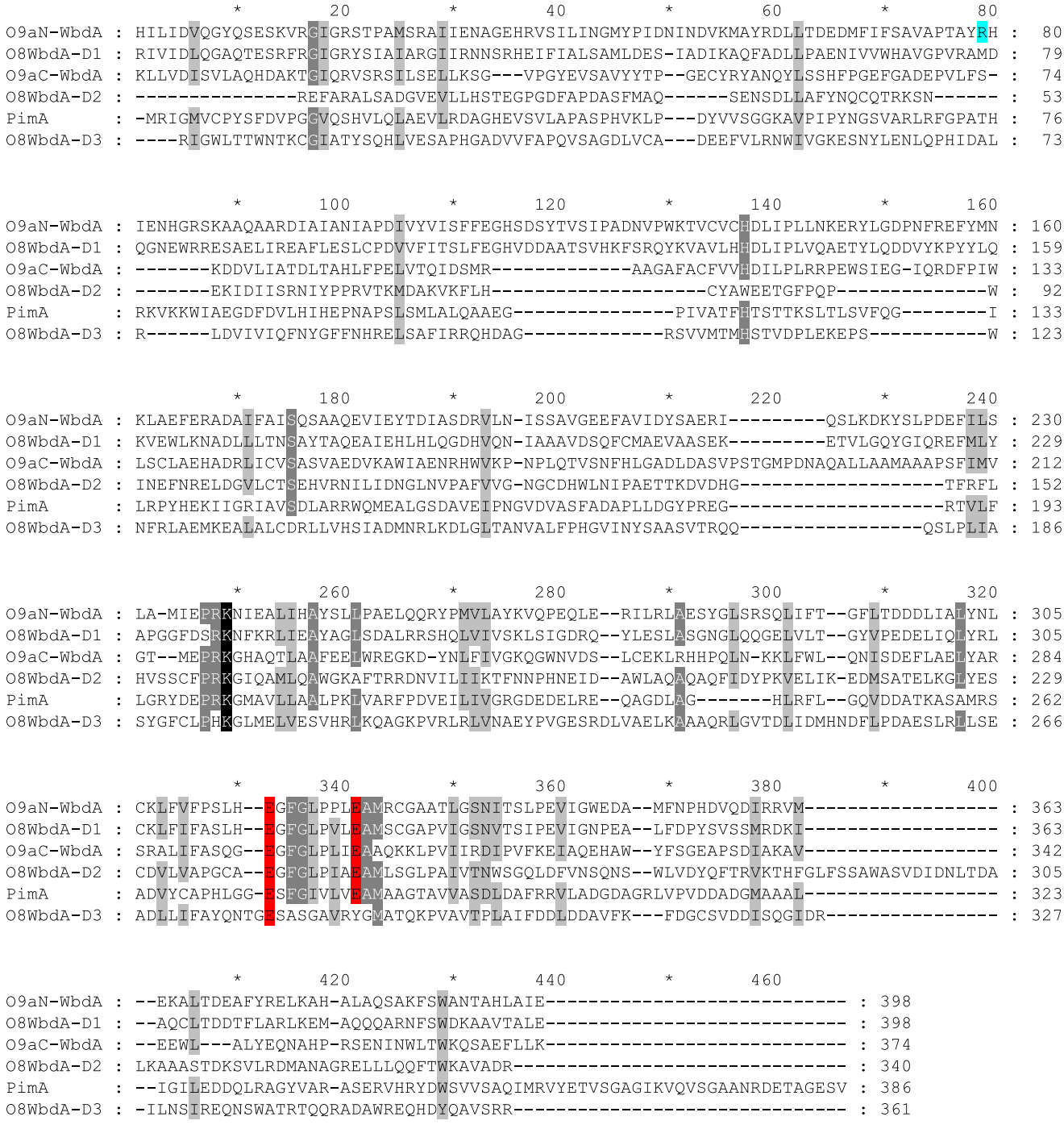


FIGURE 2. **Multiple-sequence alignment of the mycobacterial PimA α-mannosyltransferase and the O9a and O8 WbdA mannosyltransferase domains.** Conserved residues are *highlighted* in *black*, and similar residues are *highlighted* in *gray*. The Glu residues of the $EX_7E$ motifs are *highlighted* in *red*. $WbdA^{O9a}$ $Arg^{80}$ involved in the $WbdA^{O9}$ C80R O9 → O9a seroconversion is *highlighted* in *cyan*. Alignments were performed using the ClustalW2 server (28, 29).

els of the N-$WbdA^{O9a}$ and C-$WbdA^{O9a}$ domains were generated using Phyre2 (37). The highest scoring models for N-$WbdA^{O9a}$ (17% sequence identity, 91% sequence coverage, 100% confidence) and C-$WbdA^{O9a}$ (17% sequence identity, 86% sequence coverage, 100% confidence) were based on the structure of sucrose synthase 1, a GT4 enzyme from *Arabidopsis thaliana* (57). The structure of the mycobacterial PimA protein was overlaid onto the modeled structures of the $WbdA^{O9a}$ domains (Fig. 4). PimA was chosen because it is also a GDP-Man*p*-dependent mannosyltransferase belonging to the GT4 family, and its structure has been solved in complex with GDP-Man*p* (46), which may highlight possible binding interactions for the same sugar nucleotide donor in the $WbdA^{O9a}$ domains. The predicted structure of N-$WbdA^{O9a}$ and C-$WbdA^{O9a}$ closely matches PimA (Fig. 4). The typical GT-B fold (*i.e.* two loosely associated α/β/α Rossmann-like domains, separated by a linker that forms the active site cleft) is clearly evident. The Glu residues of the $EX_7E$ motifs fall within the putative active

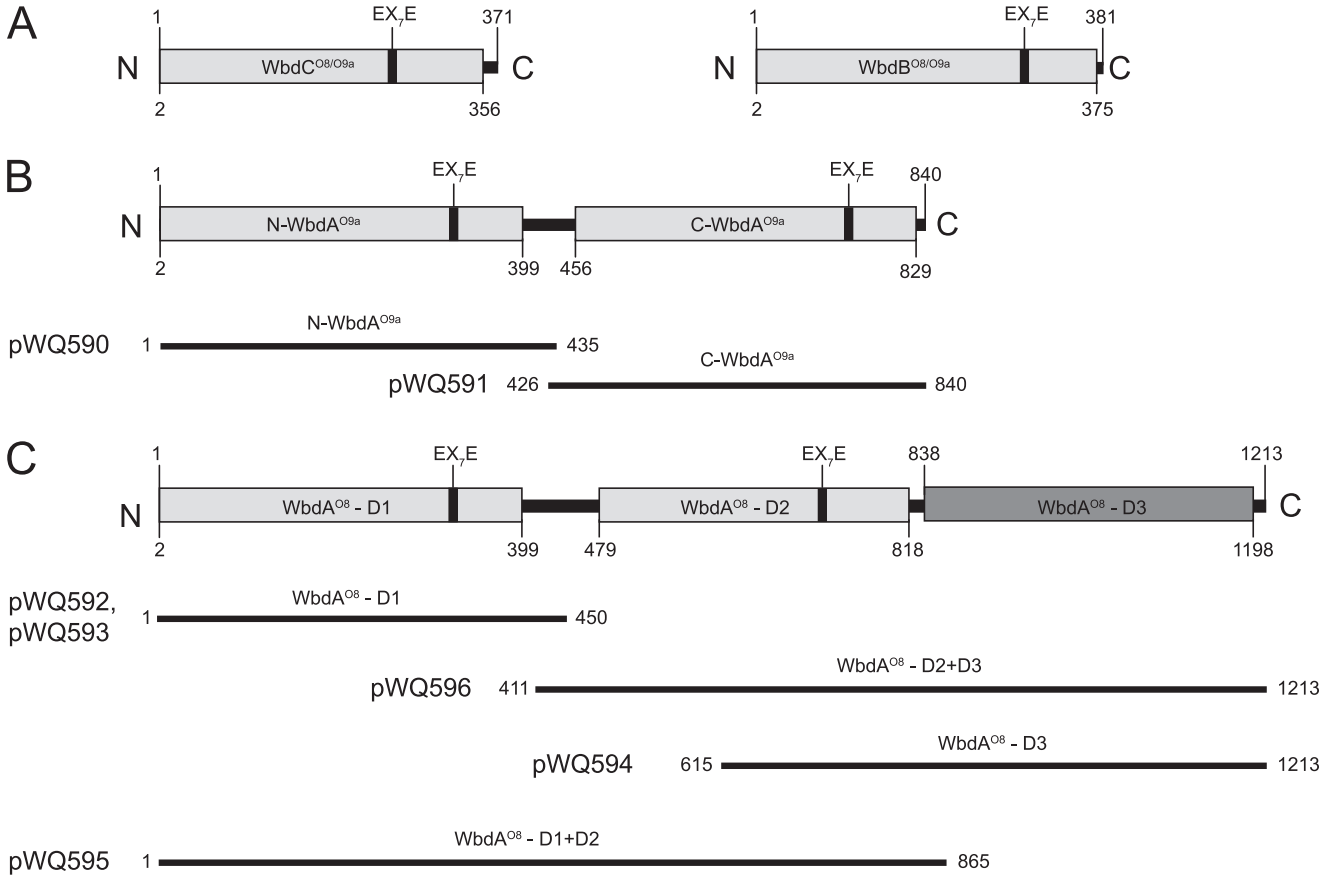


FIGURE 3. **Predicted domains of the O8 and O9a mannosyltransferases.** *A* shows WbdC$^{O8/O9a}$ and WbdB$^{O8/O9a}$, which both contain a single mannosyltransferase domain. WbdA$^{O9a}$ (*B*) contains two putative mannosyltransferase domains, and WbdA$^{O8}$ (*C*) possesses three. Domain predictions were identified using the NCBI Conserved Domain Database (24). Cloned regions encoding individual domains of the WbdA homologs are identified.

sites of N-WbdA$^{O9a}$ and C-WbdA$^{O9a}$. In N-WbdA$^{O9a}$, the Glu residues are almost superimposable on the equivalent Glu residues of the E$X_7$E motif in PimA (Fig. 4, *B* and *D*), and those of C-WbdA$^{O9a}$ also occupy a similar position. Like PimA, the carboxylate groups of the first Glu in the E$X_7$E motif of the WbdA$^{O9a}$ domains are predicted to hydrogen-bond with the Man*p* portion of GDP-Man*p*. In addition, the carboxylate groups of the second Glu are in a position to hydrogen-bond with the ribose moiety of GDP-Man*p*.

*WbdA Mannosyltransferase Domains Are Functional in Vivo When Co-expressed as Separate Domains*—Previous research indicates that the two domains of WbdA$^{O9a}$ could be expressed as independent polypeptides and rescue O9a biosynthesis in a *wbdA*::Tn*1000* mutant (26). However, interpretation of this earlier finding is complicated by the use of a transposon mutant background where *wbdA* was not completely deleted, and the extent of expression of residual parts of *wbdA* was not examined. This is a particular concern for a predicted multidomain protein. To unequivocally establish that two functional domains exist in the WbdA$^{O9a}$ protein, constructs were made with the same breakpoints in *wbdA*$^{O9a}$ used in the earlier study (26), leading to the expression of N-WbdA$^{O9a}$ and C-WbdA$^{O9a}$ (Fig. 3). From secondary structure predictions, the breakpoints fall within predicted $\alpha$-helices in a region linking the two putative glycosyltransferases domains (data not shown). Neither domain could restore O-PS production when expressed alone in a clean deletion of *wbdA*$^{O9a}$ (Fig. 5). However, when both domains were expressed as separate polypeptides, O9a O-PS biosynthesis was restored. To generate LPS products of the native size range, 0.2% L-arabinose addition was required for induction of the pBAD promoter. Therefore, as predicted, WbdA$^{O9a}$contains two separable domains, both of which are required to polymerize the O9a O-PS. In the earlier study, expression of N-WbdA$^{O9a}$ alone in the *wbdA*::Tn*1000* mutant was sufficient to generate a new polymannose glycan, whose structure differed from the O9a antigen (26). This observation could not be replicated in the Δ*wbdA*$^{O9a}$ background used here, and the disparity in the systems is addressed below.

A similar strategy was used to examine the domain architecture of WbdA$^{O8}$. The breakpoint between WbdA$^{O8}$-D1 and D2 (Fig. 3*C*) was based on the predicted domain boundaries and the predicted secondary structures in the regions linking the relevant domains (data not shown). This yielded functional constructs (Fig. 6). In contrast, the logical breakpoint identified between D2 and D3 by secondary structure prediction did not result in a functional isolated D3 domain. Several non-functional constructs were examined with nested breakpoints (data not shown). Ultimately, a conservative construct, ending partway into the adjacent D2 domain, proved to be functional. In the absence of any one of the domains, O-PS biosynthesis could not be restored in the Δ*wbdA*$^{O8}$ mutant (Fig. 6). However, O8 synthesis was rescued whenever all three domains were pres-

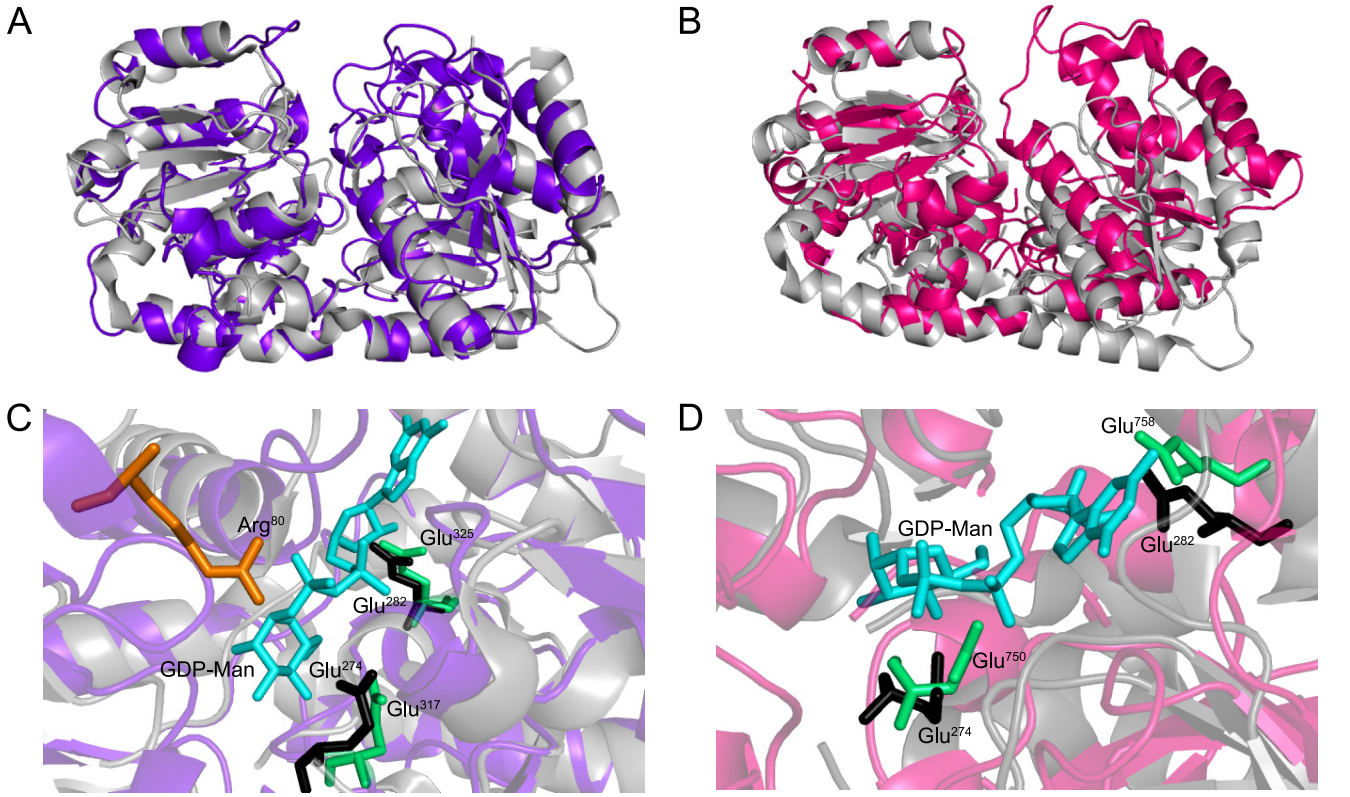


FIGURE 4. **Structural models of N-WbdA$^{O9a}$ and C-WbdA$^{O9a}$ compared with the mycobacterial PimA mannosyltransferase.** *A* and *B* show an overlay of the N-WbdA$^{O9a}$ model (*purple*) and C-WbdA$^{O9a}$ model (*magenta*) with PimA (*gray*), respectively. *C* and *D* show *expanded views* of the corresponding modeled active sites. Glu residues of the WbdA E$X_7$E motifs are *colored green*. Arg$^{80}$ is involved in the Wbd$^{O9}$ C80R O9 → O9a seroconversion (76) and is *highlighted* in *orange* in the N-WbdA$^{O9a}$ model. The Glu residues of the E$X_7$E motif in PimA are in *black*, and GDP-Man*p* is shown in *cyan*. The first Glu residue of the E$X_7$E motif is in a position to hydrogen-bond with the Man*p* moiety of GDP-Man*p*. The second Glu residue of the motif is in a position to hydrogen-bond with the ribose moiety of GDP-Man*p*.

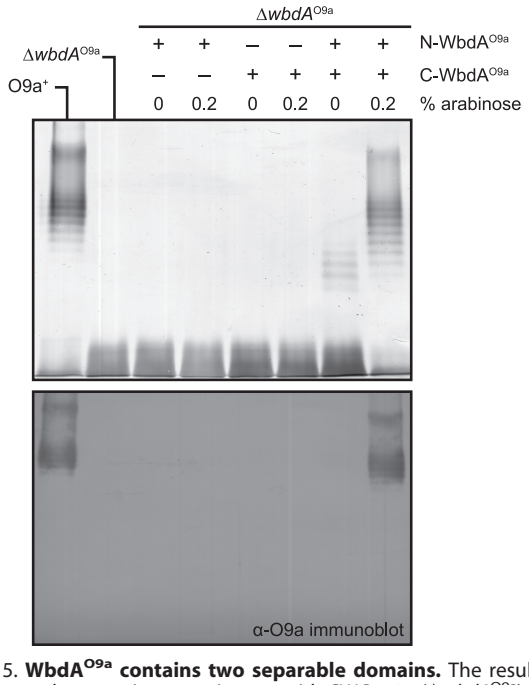


FIGURE 5. **WbdA$^{O9a}$ contains two separable domains.** The results show mutant complementation experiments with CWG1105 (Δ*wbdA*$^{O9a}$) expressing N-WbdA$^{O9a}$ (pWQ590), C-WbdA$^{O9a}$ (pWQ591), or N-WbdA$^{O9a}$ and C-WbdA$^{O9a}$ combined (pWQ590 + pWQ591). *Top*, silver-stained SDS-polyacrylamide gel of LPS samples from whole-cell lysates; *bottom*, the corresponding Western immunoblot using O9a-specific antiserum. Native O-PS biosynthesis was restored only when both WbdA$^{O9a}$ domains were present.

ent, regardless of the combination. Thus, like WbdA$^{O9a}$, WbdA$^{O8}$ appears to contain separable active domains, all of which are essential for serotype-specific O-PS biosynthesis.

*The First Glu Residue of the E$X_7$E Motif Is Crucial for the Activity of WbdC$^{O9a}$ and WbdB$^{O9a}$*—Mutagenesis studies involving several members of the GT4 family confirm the importance of the E$X_7$E motif in enzyme activity, but there is contradictory literature concerning the relative importance of each Glu residue (58–62). In the majority of cases, the first Glu appears to be more important for enzyme activity. Site-directed mutagenesis was used to investigate the importance of the E$X_7$E Glu residues in mannosyltransferases from the O8 and O9a systems, focusing initially on the single-active site enzymes, WbdC and WbdB. Four mutant constructs were generated: MalE-WbdC$^{O9a}$ E275A, MalE-WbdC$^{O9a}$ E283A, MalE-WbdB$^{O9a}$ E294A, and MalE-WbdB$^{O9a}$ E302A. Their activities were confirmed *in vivo* by assessing their ability to complement the corresponding Δ*wbdC* and Δ*wbdB* mutants (Fig. 7). In both cases, complementation was evident without induction, reflecting a leaky promoter (63). The amounts of O-PS-substituted LPS decreased with higher levels of expression following isopropyl β-D-1-thiogalactopyranoside induction. This has been observed previously with wild type genes (13), but although the reasons are unknown, this phenomenon does not affect interpretation of the complementation data. The MalE-WbdC$^{O9a}$ E275A and MalE-WbdB$^{O9a}$ E294A mutants showed a drastic reduction in activity; only trace amounts of O-PS were pro-

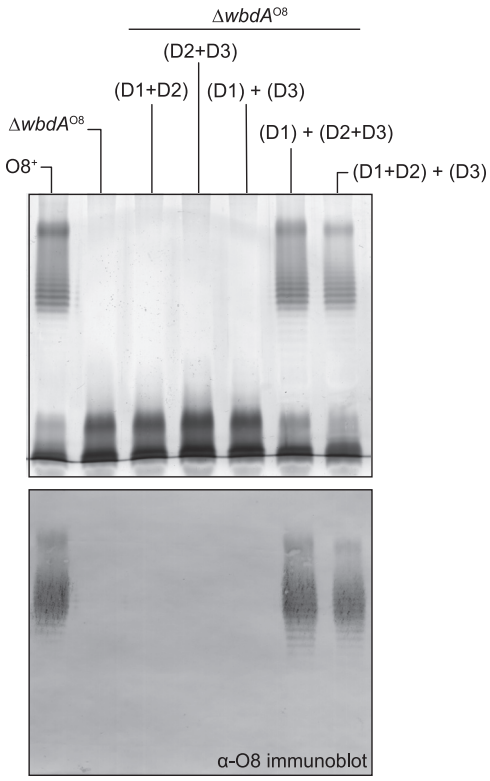


FIGURE 6. **WbdA$^{O8}$ contains three separable domains.** The results show mutant complementation experiments with CWG1104 (Δ*wbdA*$^{O8}$) expressing WbdA$^{O8}$-D1+D2 (pWQ595), WbdA$^{O8}$-D2+D3 (pWQ596), WbdA$^{O8}$-D1+D3 (pWQ593 + pWQ594), or WbdA$^{O8}$-D1+D2+D3 (pWQ592 + pWQ596 or pWQ594 + pWQ595). *Top*, silver-stained SDS-polyacrylamide gel of LPS samples from whole-cell lysates; *bottom*, the corresponding Western immunoblot using O8-specific antiserum. Native O-PS biosynthesis was restored only when all three WbdA$^{O8}$ domains were present.

duced in the presence of isopropyl β-D-1-thiogalactopyranoside inducer, and detection was only possible in the Western immunoblots. In contrast, when MalE-WbdC$^{O9a}$ E283A and MalE-WbdB$^{O9a}$ E302A were introduced into the corresponding deletion mutants, the wild type LPS profiles were restored, and detectable amounts of the O9a antigen were evident even in the absence of inducer. In all complementation experiments, the levels of protein expression were comparable with those observed when the deletion strains were transformed by constructs encoding the wild type genes (data not shown), indicating that the results were not influenced by poor expression or protein degradation. CD spectra of the MalE-WbdC$^{O9a}$ E275A and MalE-WbdB$^{O9a}$ E294A proteins were comparable with those of the wild type enzymes (data not shown), ruling out any problems with folding. These results suggest that the first Glu residue of the E$X_7$E motif plays an important role in the function of the WbdC and WbdB enzymes. In contrast, the second Glu is not essential for activity and O-PS synthesis *in vivo*, at least under the experimental conditions employed here.

*Differential Effects of Mutations in the EX$_7$E Motifs in WbdA$^{O9a}$*—To investigate the importance of the Glu residues in the EX$_7$E motif of the N-WbdA$^{O9a}$ domain, the mutant derivatives WbdD*A$^{O9a}$ E317A and WbdD*A$^{O9a}$ E325A were generated. The constructs used in these experiments contained the C-terminal portion of WbdD$^{O9a}$ (D*, representing residues 475–708), which is responsible for targeting WbdA$^{O9a}$ to the membrane (64). Co-expression of this fragment of WbdD was intended to maximize the potential association of the WbdA domain(s) with the membrane for optimal O-PS synthesis. The approach was successful. O-PS production by WbdD*A$^{O9a}$ was greater than when compared with the level of O-PS produced by the corresponding constructs lacking the C-terminal region of WbdD (data not shown).

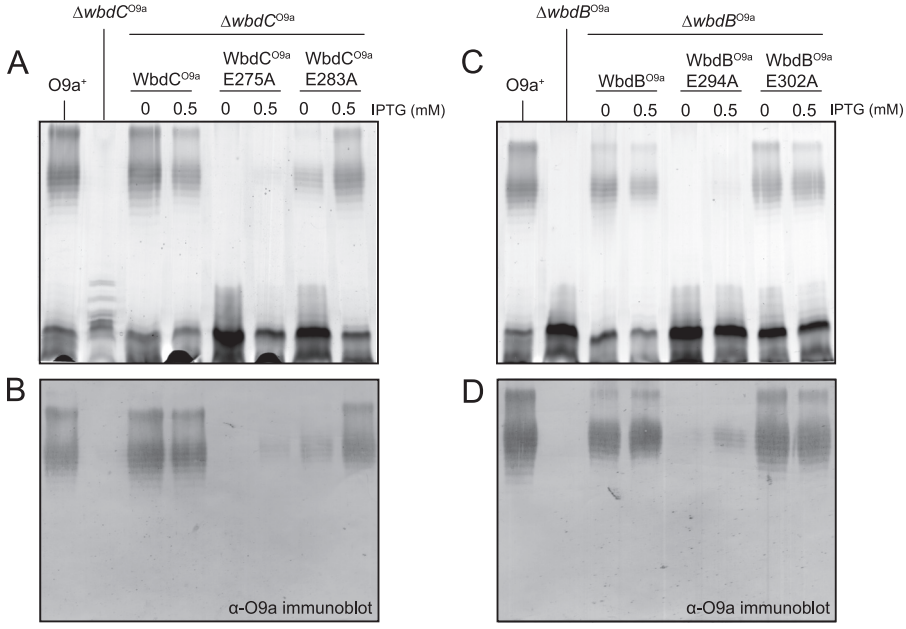


FIGURE 7. **Mutagenesis of Glu residues in the EX$_7$E motifs of WbdC$^{O9a}$ and WbdB$^{O9a}$.** The results show mutant complementation experiments with CWG1010 (Δ*wbdC*$^{O9a}$) expressing WbdC$^{O9a}$ (pWQ575), WbdC$^{O9a}$ E275A (pWQ583), or WbdC$^{O9a}$ E283A (pWQ584) (*A* and *B*) and CWG1009 (Δ*wbdB*$^{O9a}$) expressing WbdB$^{O9a}$ (pWQ576), WbdB$^{O9a}$ E294A (pWQ583), or WbdB$^{O9a}$ E302A (pWQ584) (*C* and *D*). *Top panels*, silver-stained SDS-polyacrylamide gel of LPS samples from whole-cell lysates; *bottom panels*, the corresponding Western immunoblots using O9a-specific antiserum. O-PS biosynthesis was severely impaired when only the first Glu residues of the EX$_7$E motif were substituted in WbdC$^{O9a}$ and WbdB$^{O9a}$. *IPTG*, isopropyl β-D-1-thiogalactopyranoside.

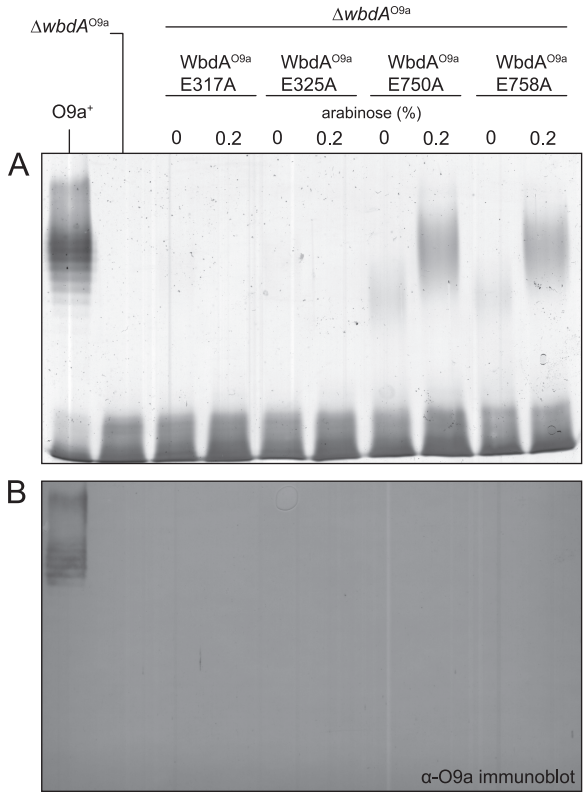


FIGURE 8. **Differential effects of mutations in the E$X_7$E motifs of WbdA$^{O9a}$.** The results show gene complementation experiments of CWG1105 (Δ*wbdA*$^{O9a}$) expressing WbdA$^{O9a}$ E317A (pWQ597), WbdA$^{O9a}$ E325A (pWQ598), WbdA$^{O9a}$ E750A (pWQ599), or WbdA$^{O9a}$ E758A (pWQ630). *A*, silver-stained SDS-polyacrylamide gel of LPS samples from whole-cell lysates; *B*, the corresponding Western immunoblot using O9a-specific antiserum. The E317A and E325A mutants were unable to support biosynthesis of O-PS, whereas the E750A and E758A mutant forms resulted in the production of O-PS with an altered structure and antigenicity.

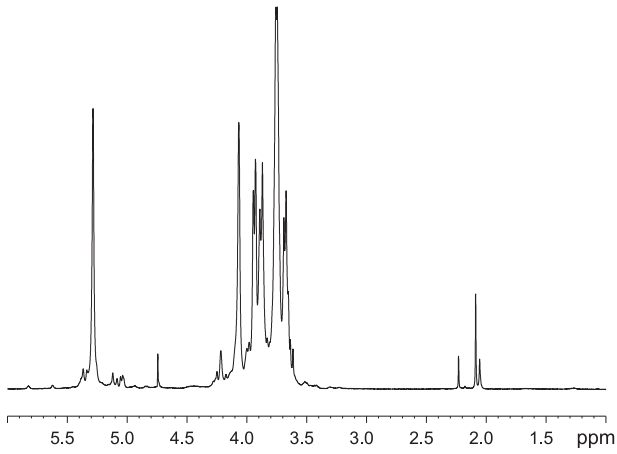


FIGURE 9. **CWG901 (Δ*wbdA*$^{O9a}$) cells expressing WbdA$^{O9a}$ E750A produce a (poly-)α-(1→2)-Man*p* O-PS.** Shown is the $^1$H NMR spectrum for purified LPS substituted with O-PS generated by *E. coli* CWG901 transformed with pWQ599.

The E317A and E325A mutant forms of WbdA$^{O9a}$ were unable to support biosynthesis of O-PS when expressed in Δ*wbdA*$^{O9a}$ (Fig. 8), indicating that both Glu residues of the N-WbdA$^{O9a}$ E$X_7$E motif are essential for the activity of the enzyme. In contrast, O-PS was produced (evident in high molecular weight LPS in silver-stained PAGE) when mutants in the C-terminal E$X_7$E motif, WbdD*A$^{O9a}$ E750A and WbdD*A$^{O9a}$ E758A, were assessed in Δ*wbdA*$^{O9a}$ (Fig. 8). However, these molecules lacked the typical "ladder-like" appearance of the native O9a LPS, and they were not detected in Western immunoblots using antibodies specific for the O9a O-PS (Fig. 8*B*), indicating altered structure and antigenicity.

To determine the structure of the novel O-PS resulting from defects in the C-terminal E$X_7$E motif, the LPS from Δ*wbdA*$^{O9a}$ expressing WbdA$^{O9a}$ E750A was purified and analyzed by NMR spectroscopy. The polysaccharide consisted of a single major monosaccharide, which was identified as α-Man*p*, based on its characteristic TOCSY pattern (data not shown). The major signals from the repeat unit domain of the glycan were indicative of a Man*p* homopolymer containing only α-(1→2) linkages (Fig. 9). The α-(1→2) linkages could not be definitively proven by NOE because intraring H-1:H-2 NOEs are always present; therefore, the substitution position was deduced from the low field chemical shift of C-2. The proposed structure is consistent with the prediction of the CASPER program (65, 66) (Table 2). This software predicts $^1$H and $^{13}$C chemical shifts from a database built from mono-, di-, and trisaccharides. This structure is consistent with the observed "smearing" pattern on the silver-stained SDS-polyacrylamide gel (Fig. 8). The typical banding pattern is generated by a heterogeneous mixture of LPS molecules on the surface of the cell that differ in length by one repeat unit in the O-PS. The lack of resolution of individual O-PS-substituted molecules is anticipated when the size increment is a single monosaccharide.

*N-WbdA$^{O9a}$ Synthesizes a Poly-α-(1→2)-Man*p* Glycan Using Synthetic Acceptor Analogues*—To investigate the potential mannosyltransferase activity of each WbdA$^{O9a}$ domain, the individual N-terminal polyhistidine-tagged WbdA$^{O9a}$ domains were purified, and their ability to transfer Man*p* residues from GDP-Man*p* to the synthetic Acceptors A and B was examined. Under the same reaction conditions, full-length WbdA$^{O9a}$ adds multiple Man*p* residues to these acceptors to generate a glycan containing the authentic O9a repeat unit (13). N-WbdA$^{O9a}$ was able to transfer multiple Man*p* residues to both acceptors (Fig. 10*A*). MALDI MS of the products formed with Acceptor B revealed the addition of up to nine Man*p* residues (Fig. 10*B*). The smallest species (*m/z* 1570.1) corresponds to the sodium adduct of the acceptor plus three additional Man*p* residues, whereas the largest (*m/z* 2542.3) is consistent with nine added Man*p* residues. The major peaks were separated by a mass difference corresponding to one Man*p* residue (162.1). Unmodified acceptor (*m/z* 1061) was not evident in the spectrum, indicating that all of the starting material was converted into product.

To determine whether a single mannosyltransferase activity or both α-(1→2)- and α-(1→3)-mannosyltransferase activities belong to N-WbdA$^{O9a}$, NMR spectroscopy was used to determine the structure of the glycan product generated by N-WbdA$^{O9a}$ using Acceptor B. The one-dimensional $^1$H spectrum revealed five anomeric resonances that integrate in a 1:1:3:1:1 ratio (Fig. 11*A*). By comparing with the CASPER database (65, 66), we see that the chemical shifts for the anomeric protons and carbons for the major product closely match those predicted for an octasaccharide with the following structure: α-Man*p*-(1→2)-α-Man*p*-(1→2)-α-Man*p*-(1→2)-α-Man*p*-(1→2)-α-Man*p*-

**TABLE 2**

**Comparison of the chemical shifts for the anomeric protons and carbons of the product generated by N-WbdA$^{O9a}$ using Acceptor B with those predicted by the CASPER database for the octasaccharide shown**

**A B C D E F**
α-Man*p*-(1→2)-α-Man*p*-(1→2)-α-Man*p*-(1→2)-α-Man*p*-(1→2)-α-Man*p*-(1→2)-α-Man*p*-(1→3)-

**G H**
α-Man*p*-(1→3)-β-Glc*p*NAc

| | A | B | C, D, E[a] | F | G | H |
|---|---|---|---|---|---|---|
| Experimental $\delta_H$ (ppm) | 5.05 | 5.30 | 5.29 | 5.34 | 5.22 | –[b] |
| CASPER $\delta_H$ (ppm) | 5.06 | 5.29 | 5.27 | 5.33 | 5.22 | 4.74 |
| Experimental $\delta_C$[c](ppm) | 103.1 | 101.4 | 101.4 | 101.5(8) | 101.6(5) | 92.6[d] |
| CASPER $\delta_C$ (ppm) | 102.9 | 101.3 | 101.2 | 101.2 | 101.5 | 95.7 |

[a] The signals for 1C, 1D, and 1E all overlap and are reported together. There are no differences in the CASPER prediction.
[b] The HOD peak at 4.76 ppm is too large to see the anomeric signal for β-D-Glc*p*NAc in the one-dimensional $^1$H spectrum.
[c] The experimental values for the $^{13}$C chemical shifts were determined from the $^1$H-$^{13}$C gHSQC spectrum (supplemental Table S1).
[d] Weak signal in the $^1$H-$^{13}$C gHSQC spectrum.

(1→2)-α-Man*p*-(1→3)-α-Man*p*-(1→3)-β-Glc*p*NAc (Table 3). This structure reflects the trisaccharide acceptor, extended by the addition of five α-(1→2)-linked Man*p* residues. gCOSY and tROESY experiments were performed and confirmed the identity of the product (Fig. 11). The resonances for H2 and H3 for each of the residues could be correlated with each anomeric signal from the gCOSY spectrum. This information was used to interpret the tROESY spectrum and assign the linkages. Key correlations from the tROESY are labeled in Fig. 11*C*. The anomeric signal at 5.34 ppm correlated with a signal at 3.84 ppm, which was assigned as the H3 proton in the same residue as the signal at 5.22 ppm. This correlation is indicative of a (1→3)-linked moiety. The anomeric signal at 5.30 ppm had an NOE correlation to a resonance at 4.08 ppm. This signal was assigned to H2 on one of the residues with the anomeric proton at 5.29 ppm, and the correlation is consistent with a (1→2)-linked residue. The anomeric signal at 5.29 ppm correlated with a signal at 4.07 ppm, which is proton H2 on the same ring as the signal at 5.34 ppm. This NOE correlation indicates another (1→2) linkage. The final key correlation is seen between the anomeric proton at 5.05 ppm and a resonance at 4.11 ppm. This signal was assigned to H2 on the same residue as the anomeric proton at 5.30 ppm and is also consistent with a (1→2) linkage. Together, these data demonstrate that N-WbdA$^{O9a}$ possesses poly-α-(1→2)-mannosyltransferase activity and generates the same α-(1→2)-linked polymannan seen *in vivo* with the full-length WbdA$^{O9a}$ derivative mutated in the C-terminal E$X_7$E motif.

In contrast to the N-terminal domain, C-WbdA$^{O9a}$ was unable to transfer Man*p* residues to either of the synthetic acceptors (Fig. 10*A*). No differences were observed between the number of residues transferred by N-WbdA$^{O9a}$ alone and the number transferred in combination with C-WbdA$^{O9a}$ (data not shown). The one-dimensional $^1$H, gCOSY, and tROESY spectra for the product generated by N-WbdA$^{O9a}$ and C-WbdA$^{O9a}$ combined in the same reaction and N-WbdA$^{O9a}$ alone were indistinguishable (data not shown). These results indicate that the product synthesized by the combined N-WbdA$^{O9a}$ and

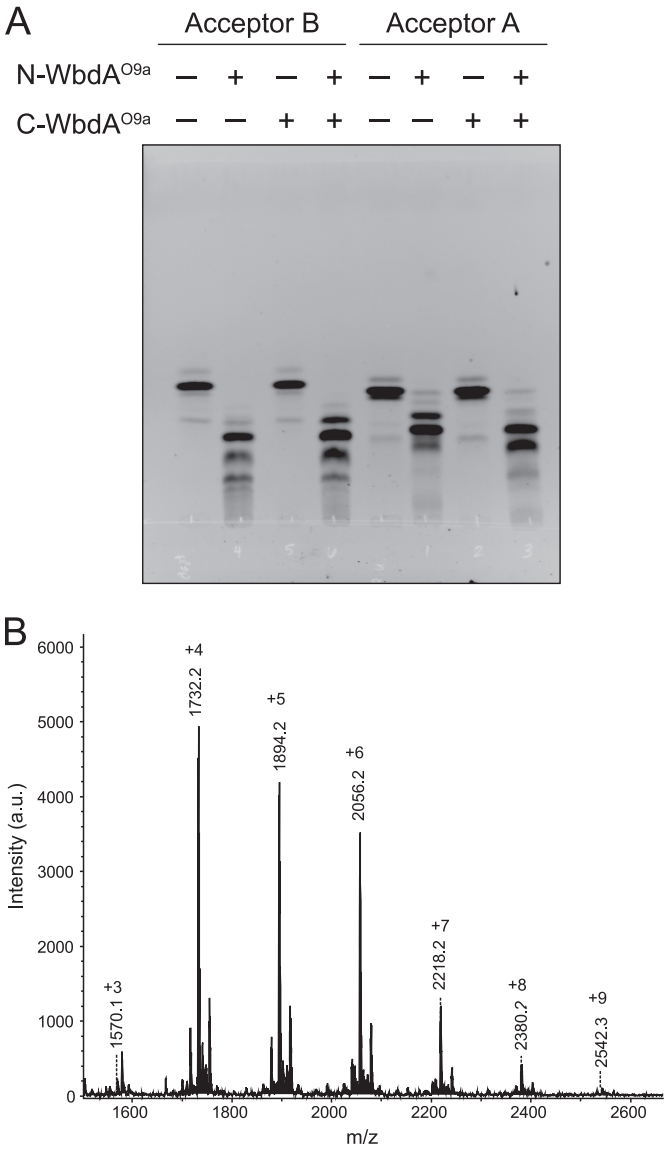


FIGURE 10. **Analysis of the *in vitro* products generated by N-WbdA$^{O9a}$ using synthetic acceptors.** The reaction products were separated by thin layer chromatography (*A*), using the fluorescein tag on the acceptors for detection. Note that C-WbdA$^{O9a}$ did not modify either acceptor; nor did its inclusion change the product profile obtained with N-WbdA$^{O9a}$. The products generated by N-WbdA$^{O9a}$ with Acceptor B were examined by MALDI MS (*B*), revealing a series of incrementally sized products that differ by the addition of one Man*p* residue. *a.u.*, arbitrary units.

C-WbdA$^{O9a}$ domains was the same α-(1→2)-linked Man*p* homopolymer seen in the presence of only N-WbdA$^{O9a}$. As described above, these same constructs are active *in vivo* and together catalyze the biosynthesis of the authentic O9a glycan. CD analysis ruled out issues associated with folding of the purified C-WbdA$^{O9a}$ domain as an explanation for its inactivity *in vitro* (data not shown).

## DISCUSSION

The mechanism of the polymerizing WbdA mannosyltransferases from *E. coli* O8 and O9a is unknown. For WbdA$^{O9a}$, a bifunctional α-(1→2)-, α-(1→3)-mannosyltransferase, the number of mannosyltransferase activities is correlated with the number of GT4 domains in the protein. This correlation also holds for the

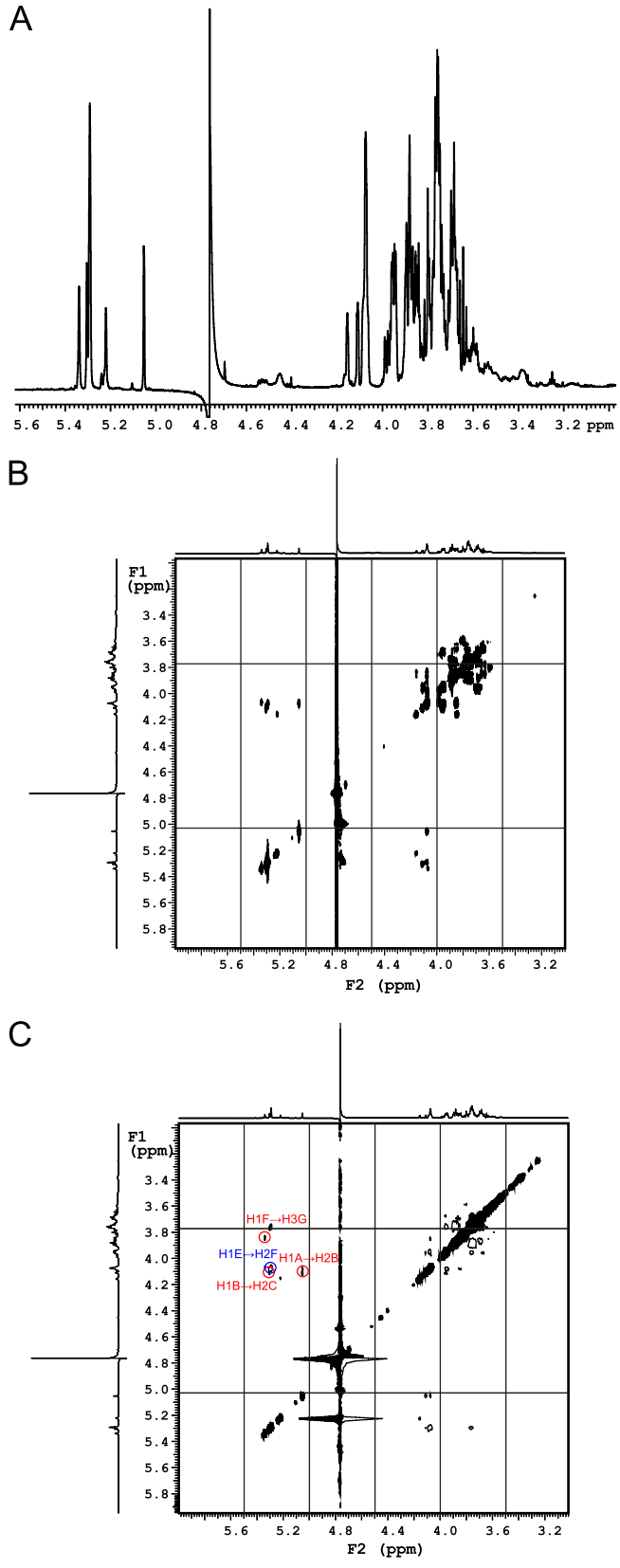


FIGURE 11. **N-WbdA$^{O9a}$ transfers Man*p* residues in α-(1→2) linkages to Acceptor B.** *A*, $^1$H NMR spectrum; *B*, gCOSY spectrum; *C*, tROESY spectrum.

trifunctional WbdA$^{O8}$ enzyme, and the most likely interpretation is that each domain contains an active site confined to one linkage type. Multidomain, bifunctional polymerases with two active sites

**TABLE 3**
**Comparison of the chemical shifts for the protons and carbons of the component Man*p* in the α-(1→2)-linked polymannose O-PS produced by CWG901 (Δ*wbdA*$^{O9a}$) cells expressing WbdA$^{O9a}$ E750A with those predicted by the CASPER database**

| | 1 | 2 | 3 | 4 | 5 | 6 |
|---|---|---|---|---|---|---|
| Experimental $\delta_H$ (ppm) | 5.28 | 4.07 | 3.93 | 3.67 | 3.75 | 3.74, 3.88 |
| CASPER $\delta_H$ (ppm) | 5.27 | 4.10 | 3.95 | 3.70 | 3.73 | 3.72, 3.88 |
| Experimental $\delta_C$ (ppm) | 101.4 | 79.6 | 70.6 | 67.7 | 73.8 | 61.8 |
| CASPER $\delta_C$ (ppm) | 101.2 | 79.1 | 70.8 | 67.8 | 74.0 | 61.8 |

have been described for hyaluronan (67, 68), chondroitin (68, 69), and heparosan (70–72) biosynthesis.

There is a solid foundation of structure-function data for the CAZy GT4 family of glycosyltransferases. Retaining-enzyme representatives, like WbdC, WbdB, and all but one domain of the WbdA homologs, possess a GT-B fold with a conserved E$X_7$E motif.[6] Crystal structures place the E$X_7$E motif within the catalytic site of the enzyme, and the consensus is that the motif is involved in binding of the nucleotide sugar donor (46, 49, 51–53). Available structures show that the two Glu residues interact with hydrogen bond donors comprising the hydroxyl groups of the sugar moiety and ribose moieties of the nucleotide sugar, respectively. The modeled structures of the N- and C-WbdA$^{O9a}$ domains superimposed on PimA suggest that the Glu residues of the WbdA$^{O9a}$ E$X_7$E motifs are likely to be involved in the binding of GDP-Man*p*. Disruption of these interactions is expected to render the domain inactive. However, there are varying results reported in the literature on the relative importance of one or both Glu residues in the E$X_7$E motif in different glycosyltransferases (46, 52, 58–62, 73). Comparison of solved structures with docked substrates will be necessary to sort out the molecular basis for the different requirements for the E$X_7$E motifs in these enzymes.

In a two-site model, each domain of WbdA$^{O9a}$ must catalyze the formation of two sequential α-(1→2) or α-(1→3) linkages. However, in the absence of a functional C-terminal active site, there is an apparent loss of control over the processivity of Man*p* transfers catalyzed by N-WbdA$^{O9a}$; *i.e.* it adds more than the two sequential α-(1→2)-linked Man*p* residues seen in the repeat unit synthesized by the full-length protein. The *in vitro* activity of N-WbdA$^{O9a}$ is entirely consistent with the *in vivo* activity of the full-length enzyme when the C-terminal active site E$X_7$E motif is mutated. One interpretation of the observed homopolymer is that competition between the active sites or interactions between the two domains in some way regulate the number of residues added. This has been observed in the bifunctional, multidomain KfoC polymerase of *E. coli* K4, which coordinates polymerization of a capsular polysaccharide with a chondroitin structure through an interaction of peptide sequences located within each domain of the enzyme (74). However, it does not preclude the additional involvement of other regulatory processes, which are generally poorly understood for the enzymes that add a defined number (two or three) of glycosyl residues in a biosynthetic pathway. For example, the *Campylobacter jejuni* PglH transfers three Gal*p*NAc residues (75), and the number of residues transferred is proposed to be controlled by the relative binding affinities of the enzyme for the growing acceptor (61). The structure of the product synthe-

sized with the synthetic acceptor and the observation that mutations in the E$X_7$E motif in the first WbdA$^{O9a}$ domain completely abolished O-PS production are consistent with the conclusion that the α-(1→2)-mannosyltransferase must precede α-(1→3) transfer in the native assembly system.

The *E. coli* O9 and O9a O-PSs are distinguished by the presence of an extra α-(1→2)-Man*p* residue in the O9 repeat unit, suggesting a change to the processivity of N-WbdA$^{O9/O9a}$ (Fig. 1). The O9 and O9a WbdA homologues share 94% identity and 97% similarity at the amino acid level. A single amino acid substitution in the WbdA$^{O9}$ homologue (C80R) is sufficient for O9 → O9a seroconversion (76). Structural modeling of N-WbdA$^{O9a}$ places Arg$^{80}$ in close proximity to the active site of N-WbdA$^{O9a}$ (Fig. 3). Based on the model, Arg$^{80}$ is unlikely to interact with the donor sugar (more than 7 Å away), although it could potentially influence other residues that do interact with the donor. It may also be in a position to form hydrogen bonds with the hydroxyl groups of the Man*p* residues in the acceptor. This could affect α-(1→2) mannosyltransferase processivity if it involves a control process similar to the one proposed for PglH (61). However, the differences between the activity of N-WbdA$^{O9a}$ *in vitro* and its role in making the authentic O9a glycan *in vivo* in the presence of C-WbdA$^{O9a}$ are suggestive of a more complex (and possibly multifactorial) regulatory process. Ultimately, a crystal structure will be necessary to resolve these questions.

Given its activity *in vitro*, the lack of *in vivo* activity of N-WbdA$^{O9a}$ is surprising. One possible explanation is that loss of some essential interactions in the absence of C-WbdA$^{O9a}$ compromises *in vivo* activity. The previous report of the formation of an α-(1→2)-linked mannan by N-WbdA$^{O9a}$ alone (26) could not be replicated here. This observation is difficult to interpret because of the uncertainty of the mutant background. Mapping data suggest that N-WbdA$^{O9a}$ and an N-terminal portion of C-WbdA$^{O9a}$ may still be expressed in the mutant. If correct, the *in vivo* α-(1→2)- mannosyltransferase activity ascribed previously to the N-WbdA$^{O9a}$ module may require a substantial portion of C-WbdA$^{O9a}$. Perhaps this region of WbdA$^{O9a}$ is involved in critical interactions with WbdD$^{O9a}$ that are responsible for the localization of the enzyme to the membrane. These interactions may not be essential when using a soluble synthetic acceptor under *in vitro* conditions.

Although all of the *in vivo* synthesis, bioinformatics, and mutagenesis data are consistent with C-WbdA$^{O9a}$ possessing α-(1→3)-mannosyltransferase activity, such activity could not be demonstrated *in vitro*. It is conceivable that C-WbdA$^{O9a}$ activity is dependent on an organized interaction with its N-WbdA$^{O9a}$ partner and that this is compromised in the absence of WbdD$^{O9a}$. The oligomeric state of WbdA$^{O9a}$ is unknown, but glycosyltransferases often form higher order oligomers (77). Proper oligomerization or multimerization (and thus function) of WbdA$^{O9a}$ may not occur in the absence of the other O9a synthesis components. WbdD$^{O9a}$ forms a trimeric structure (78), so a higher order association of WbdA$^{O9a}$ is possible through its established interaction with WbdD (64). There is precedent for the modulation of glycosyltransferase activity by inter-domain/protein interactions. In the bifunctional, multidomain *E. coli* K4 KfoC polymerase, disruption of contacts between peptides found within each domain of the enzyme results in a variant with only one active glycosyltransferase domain (74). In contrast, polymerization of the *E. coli* K5 capsular polysaccharide requires two single domain glycosyltransferases, KfiC and KfiA (79–81). KfiC is inactive in the absence of KfiA, and their interaction is proposed to cause a conformational change in KfiC, allowing it to acquire glycosyltransferase activity (81). In this context, association of the N- and C-terminal domains could change the overall structure of WbdA$^{O9a}$ to produce a bifunctional mannosyltransferase with an active conformation of C-WbdA$^{O9a}$. Conformational changes (usually upon substrate binding) are a common feature in the mechanism of glycosyltransferases and can involve the movement of flexible loops or the rotation of domains (51, 82, 83). Unlike the K5 system, *in vitro* function of C-WbdA$^{O9a}$ could not be reconstituted simply by adding N-WbdA$^{O9a}$, so the situation seems more complex. Until mannosyltransferase activity has been definitively shown for C-WbdA$^{O9a}$, alternative explanations need to be considered. One possibility is that C-WbdA$^{O9a}$ serves as a regulatory domain that alters the specificity of N-WbdA$^{O9a}$ (enabling it to switch from the transfer of Man*p* in α-(1→2) to α-(1→3) linkages). In this scenario, only N-WbdA$^{O9a}$ would be catalytically active. A similar phenomenon has been observed in the β4GT-1, the catalytic subunit of lactose synthase, where interaction with the regulatory protein α-lactalbumin alters the specificity for the acceptor substrate (84, 85). However, a parallel situation in WbdA$^{O9a}$ seems unlikely, given the high similarity shared between C-WbdA$^{O9a}$ and active GT4 enzymes as well as the functional requirement for residues in the E$X_7$E motif that are typically associated with substrate binding in systems with solved protein-substrate co-crystal structures (*e.g.* PimA (46)).

The findings reported here provide a foundation to understand the domain architecture, motifs, and other potentially important residues of the WbdA mannosyltransferases. The data reveal intriguing differences between *in vitro* and *in vivo* conditions, reflecting the sensitivity of these enzymes to their reaction environment. Collectively, these results highlight the critical requirement for defined systems to pursue both *in vivo* and *in vitro* approaches in studies such as these. The next step will be to determine the structural requirements for interactions between WbdA and WbdD in a functional complex. Understanding the structural context for the flow of alternating activities between the (putative) two catalytic sites is probably dependent on a solved structure for WbdA. Multidomain, bifunctional polymerases with two active sites have been described for hyaluronan (67, 68), chondroitin (68, 69), and heparosan (70–72) biosynthesis; thus, understanding of one system can provide molecular detail about the synthesis of a range of bioactive glycopolymers.

*Acknowledgments—We thank Dr. J. King for construction of pWQ573 and Dr. B. R. Clarke for construction of pWQ589 and pWQ631. Drs. R. Whittal and J. Zheng (Department of Chemistry Mass Spectrometry Facility, University of Alberta) provided invaluable assistance in obtaining the mass spectra of enzymatically produced products. Drs. D. Hou and C. Liu prepared Acceptors A and B.*

## REFERENCES


1. Raetz, C. R., and Whitfield, C. (2002) Lipopolysaccharide endotoxins. *Annu. Rev. Biochem.* **71,** 635–700
2. Orskov, I., Orskov, F., Jann, B., and Jann, K. (1977) Serology, chemistry, and genetics of O and K antigens of *Escherichia coli*. *Bacteriol. Rev.* **41,** 667–710
3. Stenutz, R., Weintraub, A., and Widmalm, G. (2006) The structures of *Escherichia coli* O-polysaccharide antigens. *FEMS Microbiol. Rev.* **30,** 382–403
4. Sperandeo, P., Dehò, G., and Polissi, A. (2009) The lipopolysaccharide transport system of Gram-negative bacteria. *Biochim. Biophys. Acta* **1791,** 594–602
5. Cuthbertson, L., Kos, V., and Whitfield, C. (2010) ABC transporters involved in export of cell surface glycoconjugates. *Microbiol. Mol. Biol. Rev.* **74,** 341–362
6. Greenfield, L. K., and Whitfield, C. (2012) Synthesis of lipopolysaccharide O-antigens by ABC transporter-dependent pathways. *Carbohydr. Res.* **356,** 12–24
7. Jann, K., Kanegasaki, S., Goldemann, G., and Mäkelä, P. H. (1979) On the effect of rfe mutation on the biosynthesis of the 08 and 09 antigens of *Escherichia coli*. *Biochem. Biophys. Res. Commun.* **86,** 1185–1191
8. Jann, K., Goldemann, G., Weisgerber, C., Wolf-Ullisch, C., and Kanegasaki, S. (1982) Biosynthesis of the O9 antigen of *Escherichia coli*. Initial reaction and overall mechanism. *Eur. J. Biochem.* **127,** 157–164
9. Rick, P. D., Hubbard, G. L., and Barr, K. (1994) Role of the *rfe* gene in the synthesis of the O8 antigen in *Escherichia coli* K-12. *J. Bacteriol.* **176,** 2877–2884
10. Meier-Dieter, U., Starman, R., Barr, K., Mayer, H., and Rick, P. D. (1990) Biosynthesis of enterobacterial common antigen in *Escherichia coli*. Biochemical characterization of Tn10 insertion mutants defective in enterobacterial common antigen synthesis. *J. Biol. Chem.* **265,** 13490–13497
11. Alexander, D. C., and Valvano, M. A. (1994) Role of the *rfe* gene in the biosynthesis of the *Escherichia coli* O7-specific lipopolysaccharide and other O-specific polysaccharides containing *N*-acetylglucosamine. *J. Bacteriol.* **176,** 7079–7084
12. Kido, N., Torgov, V. I., Sugiyama, T., Uchiya, K., Sugihara, H., Komatsu, T., Kato, N., and Jann, K. (1995) Expression of the O9 polysaccharide of *Escherichia coli*. Sequencing of the *E. coli* O9 *rfb* gene cluster, characterization of mannosyl transferases, and evidence for an ATP-binding cassette transport system. *J. Bacteriol.* **177,** 2178–2187
13. Greenfield, L. K., Richards, M., Li, J., Lowary, T. D., Wakarchuk, W. W., and Whitfield, C. (August 8, 2012) Biosynthesis of the polymannose lipopolysaccharide O-antigens from *Escherichia coli* serotypes O8 and O9a requires a unique combination of single- and multiple-active site mannosyltransferases *J. Biol. Chem.* 10.1074/jbc.M112.401000
14. Clarke, B. R., Cuthbertson, L., and Whitfield, C. (2004) Nonreducing terminal modifications determine the chain length of polymannose O-antigens of *Escherichia coli* and couple chain termination to polymer export via an ATP-binding cassette transporter. *J. Biol. Chem.* **279,** 35709–35718
15. Clarke, B. R., Richards, M. R., Greenfield, L. K., Hou, D., Lowary, T. L., and Whitfield, C. (2011) *In vitro* reconstruction of the chain termination reaction in biosynthesis of the *Escherichia coli* O9a O-polysaccharide. The chain length regulator, WbdD, catalyzes the addition of methyl phosphate to the non-reducing terminus of the growing glycan. *J. Biol. Chem.* **286,** 41391–41401
16. Cuthbertson, L., Kimber, M. S., and Whitfield, C. (2007) Substrate binding by a bacterial ABC transporter involved in polysaccharide export. *Proc. Natl. Acad. Sci. U.S.A.* **104,** 19529–19534
17. Reske, K., and Jann, K. (1972) The O8 antigen of *Escherichia coli*. Structure of the polysaccharide chain. *Eur. J. Biochem.* **31,** 320–328
18. Prehm, P., Jann, B., and Jann, K. (1976) The O9 antigen of *Escherichia coli*. Structure of the polysaccharide chain. *Eur. J. Biochem.* **67,** 53–56
19. Jansson, P. E., Lönngren, J., Widmalm, G., Leontein, K., Slettengren, K., Svenson, S. B., Wrangsell, G., Dell, A., and Tiller, P. R. (1985) Structural studies of the O-antigen polysaccharides of Klebsiella O5 and *Escherichia coli* O8. *Carbohydr. Res.* **145,** 59–66
20. Parolis, L. A., Parolis, H., and Dutton, G. G. (1986) Structural studies of the O-antigen polysaccharide of *Escherichia coli* 09a. *Carbohydr. Res.* **155,** 272–276
21. Saeki, A., Kido, N., Sugiyama, T., Ohta, M., Iwashita, T., Uchiya, K., and Kato, N. (1993) Isolation of *rfb* gene clusters directing the synthesis of O polysaccharides consisting of mannose homopolymers and serological analysis of lipopolysaccharides. *Microbiol. Immunol.* **37,** 601–606
22. Vinogradov, E., Frirdich, E., MacLean, L. L., Perry, M. B., Petersen, B. O., Duus, J. Ø., and Whitfield, C. (2002) Structures of lipopolysaccharides from *Klebsiella pneumoniae*. Elucidation of the structure of the linkage region between core and polysaccharide O chain and identification of the residues at the non-reducing termini of the O chains. *J. Biol. Chem.* **277,** 25070–25081
23. Kubler-Kielb, J., Whitfield, C., Katzenellenbogen, E., and Vinogradov, E. (2012) Identification of the methyl phosphate substituent at the non-reducing terminal mannose residue of the O-specific polysaccharides of *Klebsiella pneumoniae* O3, *Hafnia alvei* PCM 1223, and *Escherichia coli* O9/O9a LPS. *Carbohydr. Res.* **347,** 186–188
24. Marchler-Bauer, A., Lu, S., Anderson, J. B., Chitsaz, F., Derbyshire, M. K., DeWeese-Scott, C., Fong, J. H., Geer, L. Y., Geer, R. C., and Gonzales, N. R. (2011) CDD. A conserved domain database for the functional annotation of proteins. *Nucleic Acids Res.* **39,** D225–D229
25. Cantarel, B. L., Coutinho, P. M., Rancurel, C., Bernard, T., Lombard, V., and Henrissat, B. (2009) The Carbohydrate-Active EnZymes database (CAZy). An expert resource for glycogenomics. *Nucleic Acids Res.* **37,** D233–D238
26. Kido, N., Sugiyama, T., Yokochi, T., Kobayashi, H., and Okawa, Y. (1998) Synthesis of *Escherichia coli* O9a polysaccharide requires the participation of two domains of WbdA, a mannosyltransferase encoded within the *wb** gene cluster. *Mol. Microbiol.* **27,** 1213–1221
27. Miller, J. H. (1972) *Experiments in Molecular Genetics*, pp. 432–433, Cold Spring Harbor Laboratory, Cold Spring Harbor, NY
28. Larkin, M. A., Blackshields, G., Brown, N. P., Chenna, R., McGettigan, P. A., McWilliam, H., Valentin, F., Wallace, I. M., Wilm, A., and Lopez, R. (2007) ClustalW and ClustalX version 2.0. *Bioinformatics* **23,** 2947–2948
29. Goujon, M., McWilliam, H., Li, W., Valentin, F., Squizzato, S., Paern, J., and Lopez, R. (2010) A new bioinformatics analysis tools framework at EMBL-EBI. *Nucleic Acids Res.* **38,** W695–W699
30. Cole, C., Barber, J. D., and Barton, G. J. (2008) The Jpred 3 secondary structure prediction server. *Nucleic Acids Res.* **36,** W197–W201
31. Ouali, M., and King, R. D. (2000) Cascaded multiple classifiers for secondary structure prediction. *Protein Sci.* **9,** 1162–1176
32. Cheng, J., Randall, A. Z., Sweredoski, M. J., and Baldi, P. (2005) SCRATCH. A protein structure and structural feature prediction server. *Nucleic Acids Res.* **33,** W72–W76
33. Jones, D. T. (1999) Protein secondary structure prediction based on position-specific scoring matrices. *J. Mol. Biol.* **292,** 195–202
34. Buchan, D. W., Ward, S. M., Lobley, A. E., Nugent, T. C., Bryson, K., and Jones, D. T. (2010) Protein annotation and modeling servers at University College London. *Nucleic Acids Res.* **38,** W563–W568
35. Marchler-Bauer, A., and Bryant, S. H. (2004) CD-Search. Protein domain annotations on the fly. *Nucleic Acids Res.* **32,** W327–W331
36. Marchler-Bauer, A., Anderson, J. B., Chitsaz, F., Derbyshire, M. K., DeWeese-Scott, C., Fong, J. H., Geer, L. Y., Geer, R. C., Gonzales, N. R., Gwadz, M., He, S., Hurwitz, D. I., Jackson, J. D., Ke, Z., Lanczycki, C. J., Liebert, C. A., Liu, C., Lu, F., Lu, S., Marchler, G. H., Mullokandov, M., Song, J. S., Tasneem, A., Thanki, N., Yamashita, R. A., Zhang, D., Zhang, N., and Bryant, S. H. (2009) CDD. Specific functional annotation with the Conserved Domain Database. *Nucleic Acids Res.* **37,** D205–D210
37. Kelley, L. A., and Sternberg, M. J. (2009) Protein structure prediction on the Web. A case study using the Phyre server. *Nat. Protoc.* **4,** 363–371
38. Gasteiger, E., Hoogland, C., Gattiker, A., Duvaud, S., Wilkins, M. R., Appel, R. D., and Bairoch, A. (2005) in *The Proteomics Protocols Handbook* (Walker, J. M., eds) pp. 571–607, Humana Press, Totowa, NJ
39. Westphal, O., and Jann, J. A. (1965) in *Methods in Carbohydrate Chemistry* (Whister, R. C., ed) Vol. 5, pp. 83–91, Academic Press, Inc., New York
40. Liu, C., Skogman, F., Cai, Y., and Lowary, T. L. (2007) Synthesis of the "primer-adaptor" trisaccharide moiety of *Escherichia coli* O8, O9, and O9a lipopolysaccharide. *Carbohydr. Res.* **342,** 2818–2825

41. Hou, D., Skogman, F., and Lowary, T. L. (2008) Synthesis of 8-azidooctyl glycoside derivatives of the O-chain repeating unit of *Escherichia coli* O9a lipopolysaccharide and a methylated analog. *Carbohydr. Res.* **343,** 1778–1789
42. Hitchcock, P. J., and Brown, T. M. (1983) Morphological heterogeneity among Salmonella lipopolysaccharide chemotypes in silver-stained polyacrylamide gels. *J. Bacteriol.* **154,** 269–277
43. Laemmli, U. K. (1970) Cleavage of structural proteins during the assembly of the head of bacteriophage T4. *Nature* **227,** 680–685
44. Tsai, C. M., and Frasch, C. E. (1982) A sensitive silver stain for detecting lipopolysaccharides in polyacrylamide gels. *Anal. Biochem.* **119,** 115–119
45. Korduláková, J., Gilleron, M., Mikusova, K., Puzo, G., Brennan, P. J., Gicquel, B., and Jackson, M. (2002) Definition of the first mannosylation step in phosphatidylinositol mannoside synthesis. PimA is essential for growth of mycobacteria. *J. Biol. Chem.* **277,** 31335–31344
46. Guerin, M. E., Kordulakova, J., Schaeffer, F., Svetlikova, Z., Buschiazzo, A., Giganti, D., Gicquel, B., Mikusova, K., Jackson, M., and Alzari, P. M. (2007) Molecular recognition and interfacial catalysis by the essential phosphatidylinositol mannosyltransferase PimA from mycobacteria. *J. Biol. Chem.* **282,** 20705–20714
47. Geremia, R. A., Petroni, E. A., Ielpi, L., and Henrissat, B. (1996) Toward a classification of glycosyltransferases based on amino acid sequence similarities. Prokaryotic α-mannosyltransferases. *Biochem. J.* **318**, 133–138
48. Ruane, K. M., Davies, G. J., and Martinez-Fleites, C. (2008) Crystal structure of a family GT4 glycosyltransferase from *Bacillus anthracis* ORF BA1558. *Proteins* **73,** 784–787
49. Martinez-Fleites, C., Proctor, M., Roberts, S., Bolam, D. N., Gilbert, H. J., and Davies, G. J. (2006) Insights into the synthesis of lipopolysaccharide and antibiotics through the structures of two retaining glycosyltransferases from family GT4. *Chem. Biol.* **13,** 1143–1152
50. Chua, T. K., Bujnicki, J. M., Tan, T. C., Huynh, F., Patel, B. K., and Sivaraman, J. (2008) The structure of sucrose phosphate synthase from *Halothermothrix orenii* reveals its mechanism of action and binding mode. *Plant Cell* **20,** 1059–1072
51. Vetting, M. W., Frantom, P. A., and Blanchard, J. S. (2008) Structural and enzymatic analysis of MshA from *Corynebacterium glutamicum*. Substrate-assisted catalysis. *J. Biol. Chem.* **283,** 15834–15844
52. Batt, S. M., Jabeen, T., Mishra, A. K., Veerapen, N., Krumbach, K., Eggeling, L., Besra, G. S., and Fütterer, K. (2010) Acceptor substrate discrimination in phosphatidyl-*myo*-inositol mannoside synthesis. Structural and mutational analysis of mannosyltransferase *Corynebacterium glutamicum* PimB′. *J. Biol. Chem.* **285,** 37741–37752
53. Parsonage, D., Newton, G. L., Holder, R. C., Wallace, B. D., Paige, C., Hamilton, C. J., Dos Santos, P. C., Redinbo, M. R., Reid, S. D., and Claiborne, A. (2010) Characterization of the *N*-acetyl-α-D-glucosaminyl l-malate synthase and deacetylase functions for bacillithiol biosynthesis in *Bacillus anthracis*. *Biochemistry* **49,** 8398–8414
54. Woo, E. J., Ryu, S. I., Song, H. N., Jung, T. Y., Yeon, S. M., Lee, H. A., Park, B. C., Park, K. H., and Lee, S. B. (2010) Structural insights on the new mechanism of trehalose synthesis by trehalose synthase TreT from *Pyrococcus horikoshii*. *J. Mol. Biol.* **404,** 247–259
55. Xiang, Y., Baxa, U., Zhang, Y., Steven, A. C., Lewis, G. L., Van Etten, J. L., and Rossmann, M. G. (2010) Crystal structure of a virus-encoded putative glycosyltransferase. *J. Virol.* **84,** 12265–12273
56. Lee, S. J., Lee, B. I., and Suh, S. W. (2011) Crystal structure of the catalytic domain of cholesterol-α-glucosyltransferase from *Helicobacter pylori*. *Proteins* **79,** 2321–2326
57. Zheng, Y., Anderson, S., Zhang, Y., and Garavito, R. M. (2011) The structure of sucrose synthase-1 from *Arabidopsis thaliana* and its functional implications. *J. Biol. Chem.* **286,** 36108–36118
58. Abdian, P. L., Lellouch, A. C., Gautier, C., Ielpi, L., and Geremia, R. A. (2000) Identification of essential amino acids in the bacterial α-mannosyltransferase *aceA*. *J. Biol. Chem.* **275,** 40568–40575
59. Cid, E., Gomis, R. R., Geremia, R. A., Guinovart, J. J., and Ferrer, J. C. (2000) Identification of two essential glutamic acid residues in glycogen synthase. *J. Biol. Chem.* **275,** 33614–33621
60. Kostova, Z., Yan, B. C., Vainauskas, S., Schwartz, R., Menon, A. K., and Orlean, P. (2003) Comparative importance *in vivo* of conserved glutamate residues in the EX7E motif retaining glycosyltransferase Gpi3p, the UDP-GlcNAc-binding subunit of the first enzyme in glycosylphosphatidylinositol assembly. *Eur. J. Biochem.* **270,** 4507–4514
61. Troutman, J. M., and Imperiali, B. (2009) *Campylobacter jejuni* PglH is a single active site processive polymerase that utilizes product inhibition to limit sequential glycosyl transfer reactions. *Biochemistry* **48,** 2807–2816
62. Absmanner, B., Schmeiser, V., Kämpf, M., and Lehle, L. (2010) Biochemical characterization, membrane association, and identification of amino acids essential for the function of Alg11 from *Saccharomyces cerevisiae*, an α1,2-mannosyltransferase catalyzing two sequential glycosylation steps in the formation of the lipid-linked core oligosaccharide. *Biochem. J.* **426,** 205–217
63. Shatzman, A. R., Gross, M. S., and Rosenberg, M. (2001) in *Current Protocols in Molecular Biology*, pp. 11:16.3.1–6.3.11, John Wiley & Sons, Inc., New York
64. Clarke, B. R., Greenfield, L. K., Bouwman, C., and Whitfield, C. (2009) Coordination of polymerization, chain termination, and export in assembly of the *Escherichia coli* lipopolysaccharide O9a antigen in an ATP-binding cassette transporter-dependent pathway. *J. Biol. Chem.* **284,** 30662–30672
65. Jansson, P. E., Stenutz, R., and Widmalm, G. (2006) Sequence determination of oligosaccharides and regular polysaccharides using NMR spectroscopy and a novel Web-based version of the computer program CASPER. *Carbohydr. Res.* **341,** 1003–1010
66. Lundborg, M., and Widmalm, G. (2011) Structure analysis of glycans by NMR chemical shift prediction. *Anal. Chem.* **83,** 1514–1517
67. Jing, W., and DeAngelis, P. L. (2000) Dissection of the two transferase activities of the *Pasteurella multocida* hyaluronan synthase. Two active sites exist in one polypeptide. *Glycobiology* **10,** 883–889
68. Jing, W., and DeAngelis, P. L. (2003) Analysis of the two active sites of the hyaluronan synthase and the chondroitin synthase of *Pasteurella multocida*. *Glycobiology* **13,** 661–671
69. Sobhany, M., Kakuta, Y., Sugiura, N., Kimata, K., and Negishi, M. (2008) The chondroitin polymerase K4CP and the molecular mechanism of selective bindings of donor substrates to two active sites. *J. Biol. Chem.* **283,** 32328–32333
70. Kane, T. A., White, C. L., and DeAngelis, P. L. (2006) Functional characterization of PmHS1, a *Pasteurella multocida* heparosan synthase. *J. Biol. Chem.* **281,** 33192–33197
71. Chavaroche, A. A., van den Broek, L. A., Boeriu, C., and Eggink, G. (2012) Synthesis of heparosan oligosaccharides by *Pasteurella multocida* PmHS2 single-action transferases. *Appl. Microbiol. Biotechnol.* **95,** 1199–1210
72. Chavaroche, A. A., van den Broek, L. A., Springer, J., Boeriu, C., and Eggink, G. (2011) Analysis of the polymerization initiation and activity of *Pasteurella multocida* heparosan synthase PmHS2, an enzyme with glycosyltransferase and UDP-sugar hydrolase activity. *J. Biol. Chem.* **286,** 1777–1785
73. Kämpf, M., Absmanner, B., Schwarz, M., and Lehle, L. (2009) Biochemical characterization and membrane topology of Alg2 from *Saccharomyces cerevisiae* as a bifunctional α1,3- and 1,6-mannosyltransferase involved in lipid-linked oligosaccharide biosynthesis. *J. Biol. Chem.* **284,** 11900–11912
74. Sobhany, M., Kakuta, Y., Sugiura, N., Kimata, K., and Negishi, M. (August 30, 2012) The structural basis for a coordinated reaction catalyzed by a bifunctional glycosyltransferase in chondroitin biosynthesis. *J. Biol. Chem.* 10.1074/jbc.M112.375873
75. Glover, K. J., Weerapana, E., and Imperiali, B. (2005) *In vitro* assembly of the undecaprenyl pyrophosphate-linked heptasaccharide for prokaryotic *N*-linked glycosylation. *Proc. Natl. Acad. Sci. U.S.A.* **102,** 14255–14259
76. Kido, N., and Kobayashi, H. (2000) A single amino acid substitution in a mannosyltransferase, WbdA, converts the *Escherichia coli* O9 polysaccharide into O9a. Generation of a new O-serotype group. *J. Bacteriol.* **182,** 2567–2573
77. Hashimoto, K., Madej, T., Bryant, S. H., and Panchenko, A. R. (2010) Functional states of homooligomers. Insights from the evolution of glycosyltransferases. *J. Mol. Biol.* **399,** 196–206
78. Hagelueken, G., Huang, H., Clarke, B. R., Lebl, T., Whitfield, C., and Naismith, J. H. (2012) *Mol. Microbiol.*, in press

79. Griffiths, G., Cook, N. J., Gottfridson, E., Lind, T., Lidholt, K., and Roberts, I. S. (1998) Characterization of the glycosyltransferase enzyme from the *Escherichia coli* K5 capsule gene cluster and identification and characterization of the glucuronyl active site. *J. Biol. Chem.* **273,** 11752–11757
80. Hodson, N., Griffiths, G., Cook, N., Pourhossein, M., Gottfridson, E., Lind, T., Lidholt, K., and Roberts, I. S. (2000) Identification that KfiA, a protein essential for the biosynthesis of the *Escherichia coli* K5 capsular polysaccharide, is an α-UDP-GlcNAc glycosyltransferase. The formation of a membrane-associated K5 biosynthetic complex requires KfiA, KfiB, and KfiC. *J. Biol. Chem.* **275,** 27311–27315
81. Sugiura, N., Baba, Y., Kawaguchi, Y., Iwatani, T., Suzuki, K., Kusakabe, T., Yamagishi, K., Kimata, K., Kakuta, Y., and Watanabe, H. (2010) Glucuronyltransferase activity of KfiC from *Escherichia coli* strain K5 requires association of KfiA. KfiC and KfiA are essential enzymes for production of K5 polysaccharide, *N*-acetylheparosan. *J. Biol. Chem.* **285,** 1597–1606
82. Qasba, P. K., Ramakrishnan, B., and Boeggeman, E. (2005) Substrate-induced conformational changes in glycosyltransferases. *Trends Biochem. Sci.* **30,** 53–62
83. Breton, C., Snajdrová, L., Jeanneau, C., Koca, J., and Imberty, A. (2006) Structures and mechanisms of glycosyltransferases. *Glycobiology* **16,** 29R–37R
84. Brew, K., Vanaman, T. C., and Hill, R. L. (1968) The role of α-lactalbumin and the A protein in lactose synthetase. A unique mechanism for the control of a biological reaction. *Proc. Natl. Acad. Sci. U.S.A.* **59,** 491–497
85. Schanbacher, F. L., and Ebner, K. E. (1970) Galactosyltransferase acceptor specificity of the lactose synthetase A protein. *J. Biol. Chem.* **245,** 5057–5061
86. Guzman, L. M., Belin, D., Carson, M. J., and Beckwith, J. (1995) Tight regulation, modulation, and high-level expression by vectors containing the arabinose PBAD promoter. *J. Bacteriol.* **177,** 4121–4130
87. Cieslewicz, M., and Vimr, E. (1997) Reduced polysialic acid capsule expression in *Escherichia coli* K1 mutants with chromosomal defects in kpsF. *Mol. Microbiol.* **26,** 237–249